lymphocytes in transgenic mice expressing the viral structural genes. Biochem Biophys Res Commun 301:330–337.

Tanaka T, Kitamura F, Nagasaka Y, Kuida K, Suwa H, Miyasaka M. 1993. Selective long-term elimination of natural killer cells *in vivo* by an anti-interleukin 2 receptor beta chain monoclonal antibody in mice. J Exp Med 178:1103–1107.

Thimme R, Oldach D, Chang KM, Steiger C, Ray SC, Chisari FV. 2001. Determinants of viral clearance and persistence during acute hepatitis C virus infection. J Exp Med 194:1395–1406.

Thimme R, Bukh J, Spangenberg HC, Wieland S, Pemberton J, Steiger C, Govindarajan S, Purcell RH, Chisari FV. 2002. Viral and immunological determinants of hepatitis C virus clearance, persistence, and disease. Proc Natl Acad Sci USA 99:15661–15668.

Tseng CT, Klimpel GR. 2002. Binding of the hepatitis C virus envelope protein E2 to CD81 inhibits natural killer cell functions. J Exp Med 195:43–49.

Tsukiyama-Kohara K, Tone S, Maruyama I, Inoue K, Katsume A, Nuriya H, Ohmori H, Ohkawa J, Taira K, Hoshikawa Y, Shibasaki F, Reth M, Minatogawa Y, Kohara M. 2004. Activation of the CKI-CDK-Rb-E2F pathway in full genome hepatitis C virus-expressing cells. J Biol Chem 279:14531–14541.

Vidal-Castineira JR, Lopez ZA, Diaz PR, Alonso AR, Martinez BJ, Perez R, Fernandez SJ, Melon S, Prieto J, Rodrigo L, López LC. 2010. Effect of killer immunogloblin-like receptors in the response to combined treatment in patients with chronic hepatitis C virus infection. J Virol 84: 475–481.

Vilasco M, Larrea E, Vitour D, Dabo S, Breiman A, Reqnault B, Riezu JI, Eid P, Prieto J, Meurs EF. 2006. The protein kinase IKKepsilon can inhibit HCV expression independently of IFN and its own expression is downregulated in HCV-infected livers. Hepatology 44:1635–1647.

Wakita T, Taya C, Katsume A, Kato J, Yonekawa H, Kanegae Y, Saito I, Hayashi Y, Koike M, Kohara M. 1998. Efficient conditional transgene expression in hepatitis C virus cDNA transgenic mice mediated by the Cre/loxP system. J Biol Chem 273:9001–9006.

Yoon JC, Shiina M, Ahlenstiel G, Rehermann B. 2008. Natural killer cell function is intact after direct exposure to infectious hepatitis C virions. Hepatology 49:12–21.

European Journal of Immunology

DEAD/H BOX 3 (DDX3) helicase binds the RIG-I adaptor IPS-1 to up-regulate IFN-β-inducing potential

Hiroyuki Oshiumi, Keisuke Sakai, Misako Matsumoto and Tsukasa Seya

Department of Microbiology and Immunology, Hokkaido University Graduate School of Medicine, Kita-ku, Sapporo, Japan

Retinoic acid-inducible gene-I (RIG-I)-like receptors (RLR) are members of the DEAD box helicases, and recognize viral RNA in the cytoplasm, leading to IFN-β induction through the adaptor IFN-β promoter stimulator-1 (IPS-1) (also known as Cardif, mitochondrial antiviral signaling protein or virus-induced signaling adaptor). Since uninfected cells usually harbor a trace of RIG-I, other RNA-binding proteins may participate in assembling viral RNA into the IPS-1 pathway during the initial response to infection. We searched for proteins coupling with human IPS-1 by yeast two-hybrid and identified another DEAD (Asp-Glu-Ala-Asp) box helicase, DDX3 (DEAD/H BOX 3). DDX3 can bind viral RNA to join it in the IPS-1 complex. Unlike RIG-I, DDX3 was constitutively expressed in cells, and some fraction of DDX3 is colocalized with IPS-1 around mitochondria. The 622-662 a.a DDX3 C-terminal region (DDX3-C) directly bound to the IPS-1 CARD-like domain, and the whole DDX3 protein also associated with RLR. By reporter assay, DDX3 helped IPS-1 up-regulate IFN-β promoter activation and knockdown of DDX3 by siRNA resulted in reduced IFN-β induction. This activity was conserved on the DDX3-C fragment. DDX3 only marginally enhanced IFN-β promoter activation induced by transfected TANK-binding kinase 1 (TBK1) or I-kappa-B kinase-ε (IKKε). Forced expression of DDX3 augmented virus-mediated IFN-β induction and host cell protection against virus infection. Hence, DDX3 is an antiviral IPS-1 enhancer.

Key words: DDX3 · IFN-β · IPS-1 · RIG-I-like receptors · Viral infection

See accompanying Commentary by Mulhern and Bowie

Introduction

Retinoic acid-inducible gene-I (RIG-I) and melanoma differentiation-associated gene 5 (MDA5) are cytoplasmic RNA helicases [1–3], which signal the presence of viral RNA through the adaptor, IFN-β promoter stimulator-1 (IPS-1) (also known as mitochondrial antiviral signaling protein/caspase recruitment domain (CARD) adaptor inducing IFN-β (Cardif)/virus-induced signaling adaptor) to produce IFN-β [4–7]. IPS-1 localizes on the outer membrane of the mitochondria *via* its C-terminus [6]. Its N-terminus consists of a CARD domain, which interacts with the CARD domains of RIG-I and MDA5. Viral RNA resulting from penetration or replication are believed to assemble in the CARD-interacting helicase complex to activate the cytoplasmic IFN-inducing pathway. Although non-infected cells usually express minimal amounts of RIG-I/MDA5, the final output of type I IFN is efficiently induced at an early stage of infection to protect host cells from viral spreading.

Once IPS-1 is activated, the kinase complex consisting of TANK-homologous proteins and virus-activated kinases induce nuclear translocation of IFN regulatory factor-3 (IRF-3) to activate the IFN promoter [8]. NAK-associated protein 1, TANK-binding kinase 1 (TBK1) and I-kappa-B kinase-ε (IKKε) are components of the kinase complex that phosphorylates IRF-3 to induce type I IFN [9, 10]. RIG-I recognizes products of various RNA viruses, while MDA5 recognizes products of picornaviruses

Correspondence: Dr. Tsukasa Seya
e-mail: seya-tu@pop.med.hokudai.ac.jp

[1, 11]. RIG-I and MDA5 share the helicase domain, which is classified into the DEAD (Asp-Glu-Ala-Asp) box helicase family, and the domain can bind to various RNA structures. 5′-triphosphate RNA or short dsRNA is a ligand of RIG-I, whereas long dsRNA is a ligand of MDA5 [1, 12]. However, these RIG-I-like receptors (RLR) are usually up-regulated to a sufficient level secondary to IFN stimulation, suggesting that other molecular mechanisms are responsible for the initial sensing of viral RNA.

Here, we looked for molecules that bind IPS-1 by yeast two-hybrid, and found a DEAD box helicase, DDX3 (DEAD/H BOX 3), as a component of the complex of IPS-1. DDX3 facilitated IPS-1-mediated IFN-β induction to confer high antiviral potential on early infection phase of host cells. This is the first report showing that DDX3 is an IPS-1 complement factor for antiviral IFN-β induction in host infectious cells.

Results

Involvement of DDX3 in the IPS-1 complex

IPS-1 is constitutively present on the mitochondrial membrane and plays a central role in the cytoplasmic IFN-inducing pathway. We searched for proteins that bind IPS-1 in yeast. Using bait plasmids with the IPS-1 CARD region (aa 6–136), we screened a human lung cDNA library to isolate IPS-1 CARD-interacting proteins. We identified one clone, #62 that encodes the DDX3 C-terminal region (aa 276–662), which included partial DEAD box and helicase superfamily C-terminal regions (Fig. 1A). Their interaction was confirmed in HEK293FT cells by immunoprecipitation (IP), where DDX3 and IPS-1 were coupled (Fig. 1B). We confirmed that the C-terminal fragments of DDX3, at least 622-662 a.a, bound IPS-1 (data not shown). Taken together with the results of the yeast two-hybrid assay, the C-terminal portions of DDX3 directly bind the CARD-like region of IPS-1.

RIG-I and MDA5 helicases also bind the IPS-1 CARD domain [4]. In general, RNA helicases make a large molecular complex, and sometimes form homo- or hetero-oligomers. RIG-I binds to LGP2 helicase, and forms homo-oligomers during Sendai virus infection [11]. Hence, we examined whether DDX3 was associated with the RLR proteins by i.p. RIG-I and MDA5 co-precipitated with DDX3 (Fig. 2A), suggesting that DDX3 is involved in the complex of IPS-1 that interacts with RIG-I and/or MDA5. DDX3 bound the C-terminal helicase domain including the RD region of RIG-I (Fig. 2B). Thus, additional interaction may occur between DDX3 and RIG-I/MDA5. IPS-1 localizes to the membrane of mitochondria [6]. Three-color imaging analysis indicated that DDX3 in part co-localized to the IPS-1-mitochodria complex in non-stimulated resting HeLa cells, which express undetectable amounts of RLR (Fig. 2C and data not shown). These results together with accumulating evidence infer that non-infected cells harbor the complex of DDX3 and IPS-1 with minimal amounts of RIG-I/MDA5.

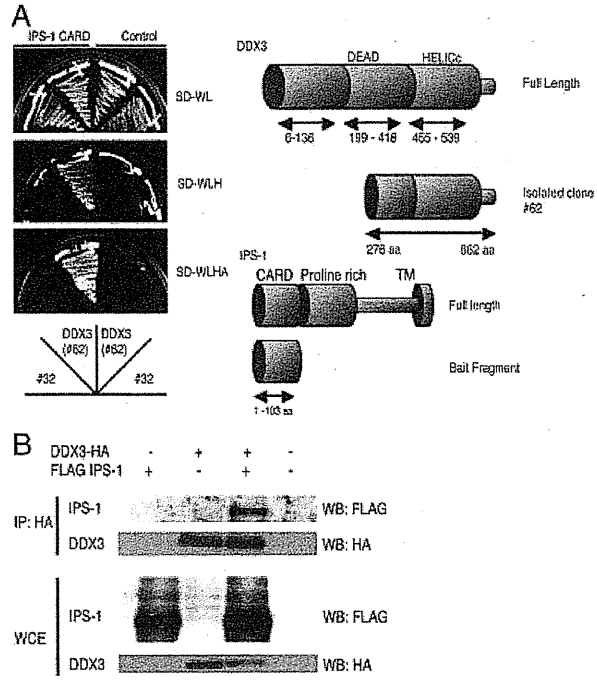

Figure 1. DDX3 binds IPS-1. (A) DDX3 partial cDNA fragment (aa 276–662) isolated by the yeast two-hybrid screening interacted with the IPS-1 CARD region (aa 1–103) in yeast. Tryptophan- and leucine-depleted synthetic dextrose medium plate (SD-WL) is non-selective, and tryptophan-, leucine- and histidine-depleted synthetic dextrose medium plate (SD-WLH) and tryptophan-, leucine-, histidine- and alanine-depleted synthetic dextrose medium (SD-WLHA) plates are selective plates. Empty bait plasmid (pGBKT7) was used for a negative control. (B) FLAG-tagged IPS-1 and HA-tagged DDX3 expression vectors were transiently transfected into HEK293FT cells by FuGeneHD reagent. 24 h after transfection, cell lysates were prepared, and IP was carried out using anti-HA Ab. The immunoprecipitates were analyzed by western blot using anti-HA or FLAG Ab. Data are representative of three independent experiments.

DDX3 promotes IPS-1-mediated IFN-β promoter activation

Forced expression of IPS-1 causes the activation of transcription from the IFN-β promoter. To ascertain the role of DDX3 in IFN-β production, we carried out reporter gene analysis to see the enhancing effect of DDX3 on IPS-1-mediated IFN-β promoter activation. Overexpression of DDX3 alone caused little activation of the promoter; however, the promoter activation was more augmented by minimal addition of DDX3 to IPS-1 than by overexpressed IPS-1 alone (Fig. 3A). This suggested that DDX3 enhanced IPS-1-mediated signaling despite the lack of RIG-I overexpression. To establish which region of DDX3 is important for IFN-β enhancer activity, partial DDX3 fragments were overexpressed with IPS-1, and IFN-β promoter activation was examined. The N-terminal region (aa 1–224, aa 224–487, aa 488–621) barely enhanced promoter activation (data not shown), but the C-terminal region (622–662) activated the promoter (Fig. 3B). These data indicated that the C-terminal region of DDX3 is important for the binding to IPS-1 and potentiation of the IPS-1 pathway.

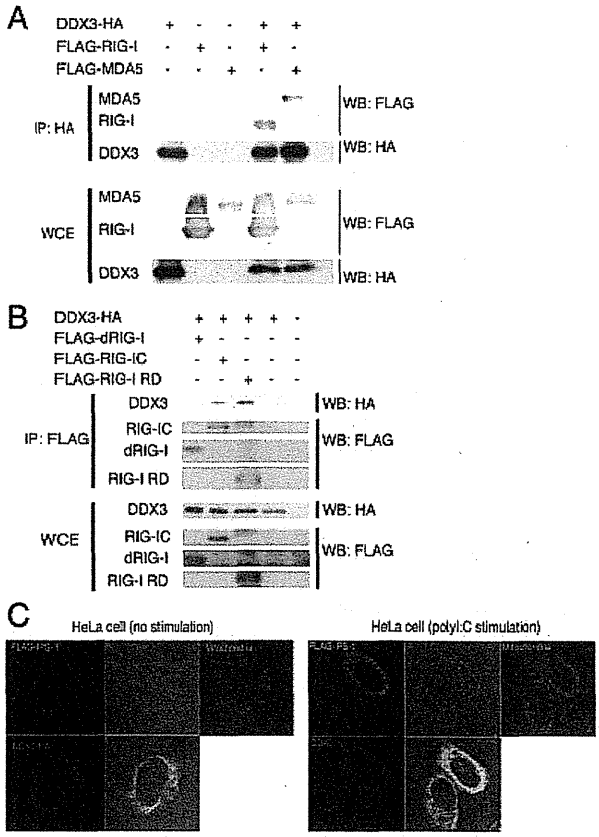

Figure 2. DDX3 joins the complex of RIG-I, MDA5 and IPS-1. (A) RIG-I and MDA5 co-precipitate with DDX3. HA-tagged DDX3 was expressed in HEK293FT cells, together with FLAG-tagged MDA5 or RIG-I, and 24 h after transfection, IP was performed using anti-HA Ab and analyzed by western blotting. (B) The C-terminal region of RIG-I participates in complex formation with DDX3. FLAG-tagged RIG-I fragments and HA-tagged DDX3 were expressed in HEK293 cells, and 24 h after transfection, IP was performed using anti-HA Ab and analyzed by western blotting. (C) DDX3 colocalizes with IPS-1. Flag-tagged IPS-1 and HA-tagged DDX3 were transfected into HeLa cells together with or without polyI:C. After 24 h, cells were fixed with formaldehyde and stained with anti-HA polyclonal and anti-FLAG monoclonal Ab. Alexa488 (DDX3-HA) or Alexa633 Ab was used for second Ab. Mitochondria was stained with Mitotracker Red. DDX-3 partially colocalized with IPS-1. Data are representative of three independent experiments.

DDX3 as a component of initial RNA sensor

RIG-I and MDA5 are IFN-inducible proteins, only traces of which exist in an early phase (<2 h) in the cytoplasm where viral RNA replicate. Previous reports showed that DDX3 binds RNA of poly rA or duplexed RNA [13, 14], and our protein analysis solidified this issue: DDX3 efficiently bound polyI:C and stem-loop RNA of viral origin in a solution (data not shown). DDX3 as well as IPS-1 were expressed even without any stimulation (Fig. 2C and 4A and B) and bound each other in the cytoplasm (Fig. 2C). Hence, DDX3 is a cytoplasmic molecule that can detect viral RNA produced in infected cells.

Knockdown studies suggested that polyI:C-mediated IFN promoter activation was abrogated in DDX3-deficient cells even in the presence of overexpressed RIG-I or MDA5 (Fig. 5). DDX3 silencing happened with two different siRNA. Thus, DDX3 may enable RIG-I and IPS-1 to confer activation of the cytoplasmic RNA-sensing pathway on virus-infected cells.

The IFN-β-inducing pathway involves IRF-3 kinases TBK1 and IKKε, which may be targets of DDX3 [15, 16]. By *in vitro* reporter analysis, increasing amounts of DDX3 barely affected IFN-β promoter activation by TBK1 and IKKε (Fig. 6A and B). Slight TBK1-enhancing activity could manage to be detected with DDX3 when decreasing amounts of TBK1 was used in the assay (Fig. 6C and D).

HeLa cells induced the mRNA of RIG-I and IFN-β in response to polyI:C stimulation within 1 h (Fig. 4A). More exactly, IFN-β induction was ~30 min faster than RIG-I induction in response to polyI:C. IFN-β mRNA induction was peaked around 3 h post stimulation, while RIG-I induction continued to increase >3 h (Fig. 4A). When HEK293 cells were infected with vesicular stomatitis virus (VSV) (a RIG-I-stimulating virus), the IFN-β mRNA was induced from 6 h, and by that time no RIG-I message was generated (Fig. 4B–D). The RIG-I message began to appear >8 h and was markedly increased (Fig. 4B and D). In either case, no up-regulation was observed with DDX3 but sufficiently present in the cytoplasm (Fig. 4C). Furthermore, overexpression of DDX3 in HeLa cells resulted in potential prevention of VSV propagation (Fig. 7). However, the distribution profiles of DDX3 and IPS-1 were barely altered in response to polyI:C stimulation (Fig. 2C). The results allow us to interpret that when viral RNA enter the cytoplasm of infected cells, the RNA first induce a small amount of IFN-β in conjunction with the complex containing trace RIG-I and then the induced IFN-β fosters intensive RIG-I/MDA5 induction. The complex is reconstituted together with upcoming RIG-I/MDA5 to amplify the cytoplasmic IFN-inducing pathway. Although the molecular reconstitution was not visible with overexpressed proteins by confocal analysis, DDX3 may act as an enhancing factor for initial RNA-sensing by the IPS-1 complex and conducts the rapid response to viral RNA to facilitate the IPS-1 signaling.

Discussion

We identified DDX3 as a protein that bound to the IPS-1 CARD region, duplexed RNA and RLR. Although the DDX3 helicase domain is a DEAD box type similar to those of RIG-I and MDA5, DDX3 does not have a signaling domain corresponding to the CARD domain. Therefore, DDX3 may not act as a signal sensor of RNA viruses, as RIG-I and MDA5 do. Considering the role of DDX3 in host RNA metabolism, it is more likely that DDX3 acts as a scaffold for RIG-I (even under the presence of low copy numbers of RIG-I) and intensifies IPS-1 signaling similar to LGP2 [11, 17]. RNA molecules usually form a complex with various

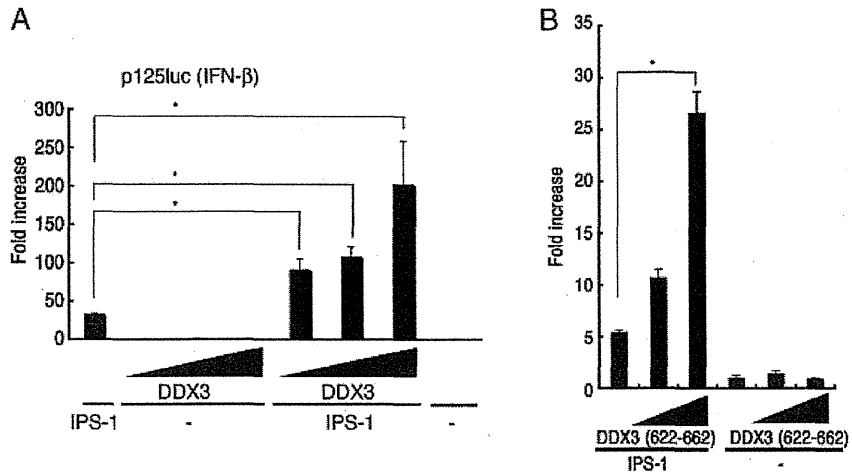

Figure 3. *The C-terminal region of DDX3 participates in enhancing IPS-1-mediated IFN-β promoter activation.* (A) Activation of IFN-β promoter was examined by reporter gene assay. HEK293 cells were transfected with DDX3- (100, 200 or 300 ng) and/or IPS-1 (100 ng)-encoding plasmids, together with reporter (p125luc) and control plasmids (Renilla luciferase) into 24-well plates. (B) The plasmids for expression of DDX3 (622-662 aa) and IPS-1 or the former only were transfected into HEK293 cells in 24-well plates together with p125luc reporter plasmid. After 24 h, the activation of reporter was measured. Data show mean fold induction+SD of three independent assays. $^{*}p<0.05$, Student's t-test.

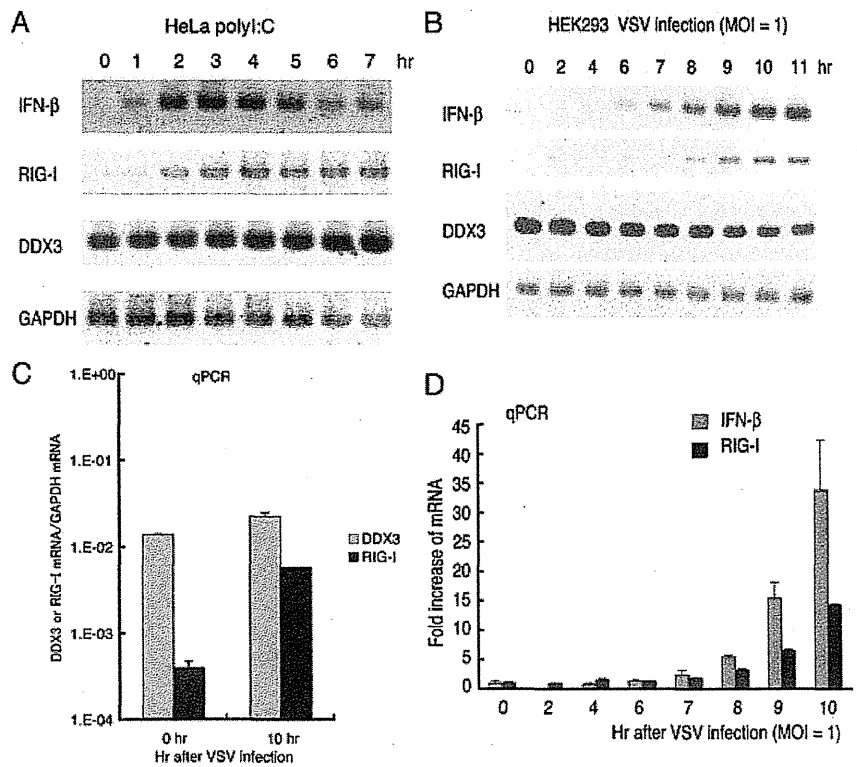

Figure 4. *Earlier induction of IFN- than RIG-I in virus-infected cells.* (A) Early induction of IFN-β in response to polyI:C. HeLa cells were stimulated with 50 μg/mL of polyI:C for indicated hours. Total RNA was extracted with TRIZOL and RT-PCR was carried out to examine the kinetics of expressions of DDX3, IFN-β, RIG-I and GAPDH (control). (B) IFN-β mRNA induction by VSV infection. HEK293 cell were infected with VSV at MOI = 1, and then total RNA was extracted with TRIZOL reagents at indicated times. The reverse transcription with random primers and PCR at 33 cycle were performed to detect RIG-I, DDX3 or IFN-β expression. Data are representative of three independent experiments. (C) Marked induction of RIG-I in VSV-infected cells. HEK293 cells were infected with VSV at MOI = 1, and then the total RNA was extracted with TRIZOL reagent at indicated times. The relative amounts of RIG-I or DDX3 mRNA were quantified by RT-qPCR, in which the mRNA of GAPDH was used for endogenous internal control. (D) Fold increase of IFN-β or RIG-I mRNA by VSV infection. The amount of IFN-β or RIG-I cDNA was determined by quantitative PCR. The fold increases were calculated by dividing the values of each time point by that of 0 h sample of IFN-β or RIG-I. Data show mean+SD pooled from three independent experiments.

proteins, such as 5′-end capping enzymes or translation initiation factors. Viral RNA also tends to couple with host proteins to replicate and translate RNA. DDX3 capturing RNA may function either in the molecular complex of RIG-I/MDA5/IPS-1 or in the complex of the translation machinery.

Recently, DDX3 was reported to up-regulate IFN-β induction by interacting with IKKε in the kinase complex [18]. IKKε is an NF-κB-inducible gene, whereas the DDX3-IPS-1 complex is constitutively present prior to infection. DDX3 may bind IKKε after IKKε is generated secondary to NF-κB activation [15]. Another report suggested that DDX3 interacts with TBK1 to synergistically stimulate the IFN-β promoter [16]. The report further suggested that DDX3 is recruited to the IFN promoter and acts like a transcription factor [16]. These reports also show that not C-terminal but N-terminal region of DDX3 is required for enhancing the IKKε- or TBK1-mediated IFN promoter activation. We showed that unlike these previous reports, the C-terminal region of DDX3 is important for the IPS-1 activation. These observations indicate that DDX3 is involved in RIG-I signaling at multiple steps. The involvement of DDX3 at several steps is not surprising, because DDX3 plays several roles in RNA metabolisms, such as RNA translocation or mRNA translation.

In cytoplasm, there are large amounts of DDX3 and only trace amounts of RIG-I in resting cells. Therefore, when the virus initially infects human cells, the viral RNA would encounter DDX3 before RIG-I capture the viral RNA. We demonstrated that the initial IPS-1 complex for RNA-sensing involves DDX3 in addition to trace RIG-I to cope with the early phase of infection. This IPS-1 complex activates downstream signal by involving a minute amount of viral RNA. What happens in actual viral infection is to first induce IFN-β and then RIG-I (Fig. 4B), suggesting that the initial IFN-β mRNA arises independent of the virus-induced RIG-I. Once IFN-β and RIG-I mRNA are up-regulated by viral RNA, the IPS-1 complex turns constitutionally different: the complex contains high amounts of RIG-I, which may directly capture viral RNA without DDX3. Our results indicate that the early IPS-1 complex formed in the early stages of virus-infected cells induce minute IFN-β with a mode different from the conventional IPS-1 pathway that RIG-I solely capture viral RNA and activates IPS-1. By retracting DDX3 from the complex by siRNA, only a minimal IFN-β response emerges merely with preexisting RIG-I and IPS-1, suggesting DDX3 to be a critical signal enhancer in the early IPS-1 complex. Development of a method to chase endogenous DDX3 will be required to test our interpretation.

The RIG-I generation occurring > 8 h post RNA virus challenge makes the complex direct the conventional IFN-inducing pathway harboring sufficient RIG-I/MDA5. Previous reports [13, 14] and our RNA-binding analysis also speculated that one of the RNA-capture proteins is DDX3 since DDX3 tightly binds polyI:C and dsRNA in fluid phase. These RNA-capture proteins may have a role in the IPS-1-involving molecular platform in cells with early virus infection when only a trace RIG-I protein is expressed. This interpretation fits the result that DDX3 acts predominantly on an early phase of virus infection (Fig. 4B and 7).

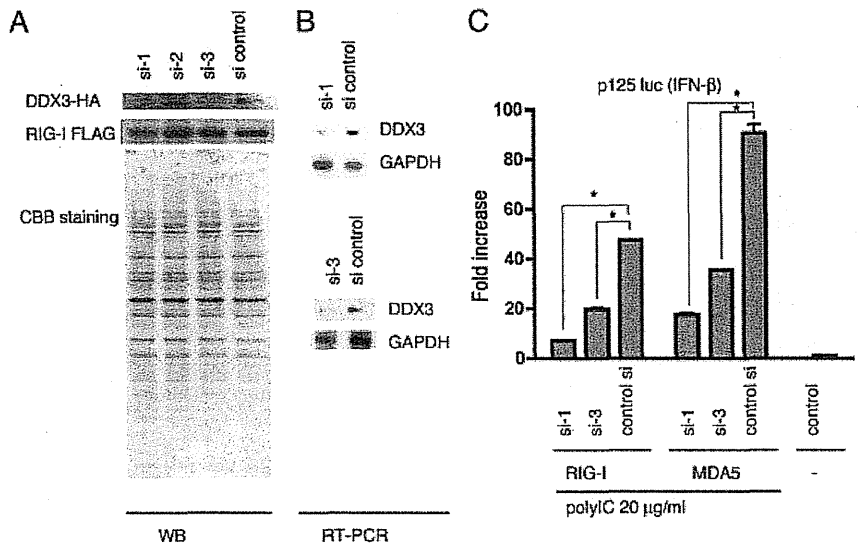

Figure 5. Knockdown of DDX3. (A) Negative control or DDX3 targeting siRNA (20 pmol), DDX3 si-1, -2 or -3, were transfected into HEK293 cells in 24-well plates, together with HA-tagged DDX3 or FLAG-tagged RIG-I expression plasmids, and after 48 h, cell lysates were prepared and analyzed by western blotting with anti-HA or anti-FLAG Ab, and the same membrane was stained with CBB. (B) DDX3 si-1, -3 or control siRNA was transfected into HEK293 cells, and after 48 h, expression of endogenous DDX3 mRNA was examined by RT-PCR. (C) DDX3 si-1, -3 or control siRNA was transfected into HEK293 cells with reporter plasmids and RIG-I- or MDA5 expression plasmid (100 ng). Forty-eight hours after transfection, cells were stimulated with polyI:C (20 μg/mL) with dextran for 4 h, and activation of the reporter was measured. siRNA for DDX3 reduced RIG-I- or MDA5-mediated p125luc activation. Data are representative of three independent experiments (A,B). Data show mean fold increase + SD pooled from three independent experiments (C). *$p<0.05$, Student's *t*-test.

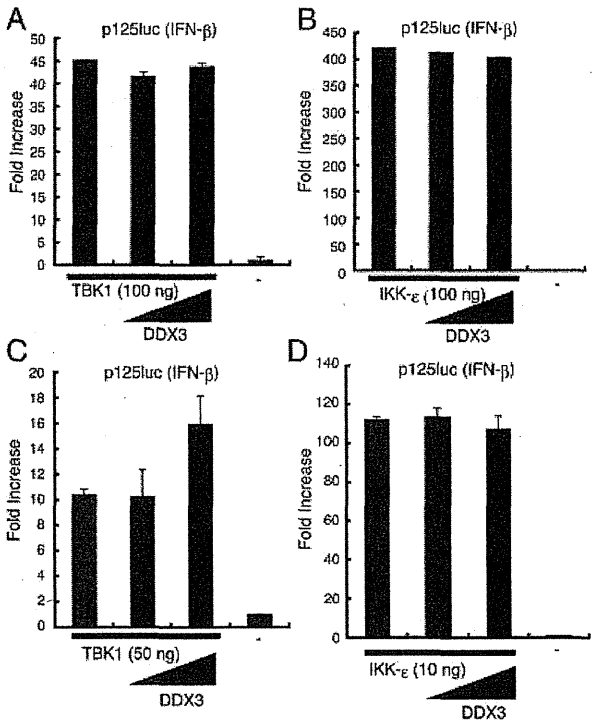

Figure 6. TBK1 and IKKε are not main targets for DDX3-mediated IFN-β up-regulation. (A–D) The activation of IFN-β promoter was examined by reporter gene assay. HEK293 cells were transfected in 24-well plates with DDX3 (0, 100 or 300 ng)-, TBK1 (0, 50 or 100 ng)- or IKKε (0, 10 or 100 ng)-encoding plasmid together with reporter (p125luc) and control plasmid. After 24 h, the cell lysate was prepared and the luciferase activities were measured. Data show mean+SD of three independent experiments.

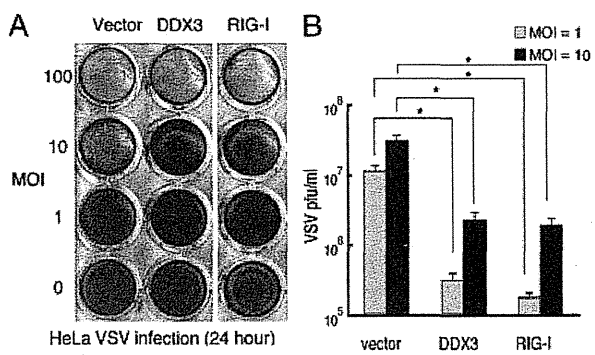

Figure 7. VSV infection is suppressed by overexpressed DDX3. (A) HeLa cells were transfected with DDX3, RIG-I or empty vector. After 24 h, the transfected cells were infected with VSV at indicated MOI. 24 h after VSV infection, the cells were fixed with formaldehyde and stained with crystal violet. (B) The VSV titers of culture supernatant of HeLa cells infected with VSV at MOI = 1 or 10 were measured by plaque assay. Data show mean+SD of three independent experiments. *$p<0.05$, Student's t-test.

Proteins involved in type I IFN induction are found ubiquitinated for their functional regulation. It has been reported that TRIM25 [19] and Riplet/RNF135 [20] act as ubiquitin ligases to activate RIG-I for IFN-β induction in their different sites of RIG-I ubiquitination. Another ubiquitin ligase RNF125 poly-ubiquitinates RIG-I through Lys48, leading to degradation of RIG-I [21]. The RIG-I level is highly susceptible to not only IFN but also ubiquitination in host cells. In addition, many viral factors may suppress the RIG-I function. It remains unknown what factor maintains a minimal level of RIG-I/MDA5 in resting cells. We favor the interpretation that DDX3 can be an alternative factor for compensating the low RLR contents in a certain infectious situation such that RIG-I is degraded or poorly up-regulated by other viral factors.

DDX3 is functionally complicated since its protective role against viruses may be modulated after the synthesis of viral proteins. DDX3 couples with the HCV core protein in HCV-infected cells and promotes viral replication [22]. This alternative function of DDX3 is accelerated by the HCV core protein, since the core protein withdraws DDX3 from the IFN-β-inducing facility, leading to suppression of IFN-β induction and positive regulation of HCV propagation in infected cells. DDX3 is also involved in HIV RNA translocation [14]. The DDX3 gene is conserved among eukaryotes, and Ded1 is a budding yeast homolog [23]. Ded1 helicase is essential for initiation of host mRNA translation, and human DDX3 can complement the lethality of Ded1-null yeast cells [24, 25]. Hence, another function of DDX3 is to bind viral RNA to modulate RNA replication and translocation. It is not surprising that DDX3 is implicated in various steps of RNA metabolism in cells with both host and viral RNA.

Materials and methods

Cell culture and reagents

HEK293 cells and HEK293FT cells were maintained in Dulbecco's Modified Eagle's low or high glucose medium (Invitrogen, Carlsbad, CA, USA) supplemented with 10% heat-inactivated FBS (Invitrogen) and antibiotics. HeLa cells were maintained in MEM (Nissui, Tokyo, Japan) supplemented with 10% heat-inactivated FBS. Anti-FLAG M2 mAb, anti-HA polyclonal Ab, were purchased from Sigma-Aldrich (St. Louis, MO, USA). Alexa Fluor®-conjugated secondary Ab were from Invitrogen.

Plasmids

DDX3 cDNA encoding the entire ORF was cloned into pCR-blunt vector using primers, DDX3N F-Xh (CTC GAG CCA CCA TGA GTC ATG TGG CAG TGG AA) and DDX3C R-Ba (GGA TCC GTT ACC CCA CCA GTC AAC CCC) from human lung cDNA library. To make an expression plasmid, HA tag was fused at the C-terminal end of the full length DDX3 (pEF-BOS DDX3-HA). pEF-BOS DDX3 (1–224 aa) vector was made by using primers DDX3 N-F-Xh and DDX3D1 (GGA TCC GGC ACA AGC CAT CAA GTC TCT TTT C).

pEF-BOS DDX3-HA (225–662) was made by using primers DDX3D2-3 (CTC GAG CCA CCA TGC AAA CAG GGT CTG GAA AAA C) and DDX3C R-Ba. To make pEF-BOS DDX3-HA (225–484) and pEF-BOS DDX3-HA (485–663), the primers DDX3D2 R-Ba (GGA TCC AAG GGC CTC TTC TCT ATC CCT C) and DDX3D3 F-Xh (CTC GAG CCA CCA TGC ACC AGT TCC GCT CAG GAA AAA G) were used, respectively. Reporter and internal control plasmids for reporter gene assay are previously described [26].

RNAi

Knockdown of DDX3 was carried out using siRNA, DDX3 siRNA-1: 5′-GAU UCG UAG AAU AGU CGA ACA-3′, siRNA-2: 5′-GGA GUG AUU ACG AUG GCA UUG-3′, siRNA-3: 5′-GCC UCA GAU UCG UAG AAU AGU-3′ and control siRNA: 5′-GGG AAG AUC GGG UUA GAC UUC-3′. Twenty picomoles of each siRNA was transfected into HEK293 cells in 24-well plates with Lipofectamin 2000 according to manufacture's protocol. Knockdown of DDX3 was confirmed 48 h after siRNA transfection. Experiments were repeated twice for confirmation of the results.

Yeast two-hybrid assay

The yeast two-hybrid assay was performed as described previously [27]. The yeast AH109 strain (Clontech, Palo Alto, CA, USA) was transformed using bait (pGBKT7) and prey (pGADT7) plasmids. The transformants were streaked onto plates and incubated for 3–5 days. The IPS-1 CARD vector was constructed by inserting IPS-1 partial fragment encoding from 6 to 136 aa region into pGBKT7 multicloning site. Yeast two-hybrid screening was performed using human lung cDNA libraries. We obtained four independent clones, and one encoded DDX3 partial cDNA. SD-WLH is a yeast synthetic dextrose medium that lacks Trp, Leu and His aa. SD-WLHA lacks adenine in addition to Trp, Leu and His. SD-WL lacks Trp and Leu and thus non-selective plate.

Reporter assay

HEK293 cells (4×10^4 cells/well) cultured in 24-well plates were transfected with the expression vectors for IPS-1, DDX3 or empty vector together with the reporter plasmid (100 ng/well) and an internal control vector, phRL-TK (Promega) (2.5 ng/well) using FuGENE (Roche) as described previously [28]. The p-125 luc reporter containing the human IFN-β promoter region (−125 to +19) was provided by Dr. T. Taniguchi (University of Tokyo, Tokyo, Japan). The total amount of DNA (500 ng/well) was kept constant by adding empty vector. After 24 h, cells were lysed in lysis buffer (Promega), and the *Firefly* and *Renella* luciferase activities were determined using a dual-luciferase reporter assay kit (Promega). The *Firefly* luciferase activity was normalized by *Renella* luciferase activity and is expressed as the fold stimulation relative to the activity in vector-transfected cells. Experiments were performed three times in duplicate (unless otherwise indicated in the legends).

PolyI:C stimulation

PolyI:C was purchased from GE Healthcare company, and solved in milliQ water. For polyI:C treatment, polyI:C (50 μg/mL) was mixed with DEAE-dextran (0.5 mg/mL) (Sigma) in the culture medium, and the cell culture supernatant was replaced with the medium containing polyI:C and DEAE-dextran. Using DEAE-dextran, polyI:C is incorporated into the cytoplasm to activate RIG-I/MDA5.

Virus preparation and infection

VSV Indiana strain or poliovirus type 1 Mahoney strain were used for virus assay. Vero derived cell (Vero-SLAM) was used for propagation and plaque assay for VSV indiana strain or poliovirus type 1 Mahoney strain. HEK293 cells were infected with viruses at MOI = 0.001 in a 24-well plate. The virus titers of culture media at indicated hours post infection in the figures were determined by plaque assay using Vero-SLAM cells. In some experiments that require rapid virus propagation, high MOI ($0.1 \sim 1$) was used for infection.

Immunoprecipitation

HEK293FT cells were transfected in a 6-well plate with plasmids encoding DDX3, IPS-1, RIG-I or MDA5 as indicated in the figures. Twenty-four hours after tranfection, the total cell lysate was prepared by lysis buffer (20 mM Tris-HCl (pH 7.5) containing 125 mM NaCl, 1 mM EDTA, 10% glycerol, 1% NP-40, 30 mM NaF, 5 mM Na3Vo4, 20 mM IAA and 2 mM PMSF), and the protein was immunoprecipitated with anti-HA polyclonal (Sigma) or anti-FLAG M2 mAb (Sigma). The precipitated samples were resolved on SDS-PAGE, blotted onto a nitrocellulose sheet and stained with anti-HA (HA1.1) monoclonal (Sigma), anti-HA polyclonal or anti-FLAG M2 mAb.

Confocal analysis

HeLa cells were plated onto cover glass in a 24-well plate. In the following day, cells were transfected with indicated plasmids using Fugene HD (Roch). The amount of DNA was kept constant by adding empty vector. After 24 h, cells were fixed with 3% of paraformaldehyde in PBS for 30 min, and then permeabilized with PBS containing 0.2% of Triton

X-100 for 15 min. For the polyI:C stimulation, 100 ng of polyI:C were transfected into HeLa cell in 24-well plates together with IPS-1 or DDX3 expressing vectors, and 24 h after the transfection, the cells were fixed and stained for confocal microscopic analysis. Permeabilized cells were blocked with PBS containing 1% BSA and were labeled with anti-Flag M2 mAb (Sigma), anti-HA polyclonal Ab (Sigma) or Mitotracker in 1% BSA/PBS for 1 h at room temperature. The cells were then washed with 1% BSA/PBS and treated for 30 min at room temperature with Alexa-conjugated Ab (Molecular Probes). Thereafter, micro-cover glass was mounted onto slide glass using PBS containing 2.3% DABCO and 50% of glycerol. The stained cells were visualized at ×60 magnification under a FLUOVIEW (Olympus, Tokyo, Japan).

Acknowledgements: The authors thank Dr. M. Sasai, Dr. T. Ebihara, Dr. K. Funami, Dr. A. Matsuo, Dr. A. Ishii, Dr. A. Watanabe and Dr. M. Shingai in our laboratory for their critical discussions. This work was supported in part by CREST and Innovation, JST (Japan Science and Technology Corporation), the Program of Founding Research Centers for Emerging and Reemerging Infectious Diseases, MEXT, Sapporo Biocluster "Bio-S," the Knowledge Cluster Initiative of the MEXT, Grants-in-Aid from the Ministry of Education, Science, and Culture (Specified Project for Advanced Research) and the Ministry of Health, Labor, and Welfare of Japan, Mitsubishi Foundation, Mochida Foundation, NorthTec Foundation and Takeda Foundation.

Conflict of interest: The authors declare no financial or commercial conflict of interest.

References

1 Kato, H., Takeuchi, O., Sato, S., Yoneyama, M., Yamamoto, M., Matsui, K., Uematsu, S. *et al.*, Differential roles of MDA5 and RIG-I helicases in the recognition of RNA viruses. *Nature* 2006. **441**: 101–105.

2 Gitlin, L., Barchet, W., Gilfillan, S., Cella, M., Beutler, B., Flavell, R. A., Diamond, M. S. *et al.*, Essential role of mda-5 in type I IFN responses to polyriboinosinic:polyribocytidylic acid and encephalomyocarditis picornavirus. *Proc. Natl. Acad. Sci. USA* 2006. **103**: 8459–8464.

3 Yoneyama, M., Kikuchi, M., Natsukawa, T., Shinobu, N., Imaizumi, T., Miyagishi, M., Taira, K. *et al.*, The RNA helicase RIG-I has an essential function in double-stranded RNA-induced innate antiviral responses. *Nat. Immunol.* 2004. **5**: 730–737.

4 Kawai, T., Takahashi, K., Sato, S., Coban, C., Kumar, H., Kato, H., Ishii, K. J. *et al.*, IPS-1, an adaptor triggering RIG-I- and Mda5-mediated type I interferon induction. *Nat. Immunol.* 2005. **6**: 981–988.

5 Meylan, E., Curran, J., Hofmann, K., Moradpour, D., Binder, M., Bartenschlager, R. and Tschopp, J., Cardif is an adaptor protein in the RIG-I antiviral pathway and is targeted by hepatitis C virus. *Nature* 2005. **437**: 1167–1172.

6 Seth, R. B., Sun, L., Ea, C. K. and Chen, Z. J., Identification and characterization of MAVS, a mitochondrial antiviral signaling protein that activates NF-kappaB and IRF 3. *Cell* 2005. **122**: 669–682.

7 Xu, L. G., Wang, Y. Y., Han, K. J., Li, L. Y., Zhai, Z. and Shu, H. B., VISA is an adapter protein required for virus-triggered IFN-beta signaling. *Mol. Cell* 2005. **19**: 727–740.

8 Sasai, M., Matsumoto, M. and Seya, T., The kinase complex responsible for IRF-3-mediated IFN-beta production in myeloid dendritic cells (mDC). *J. Biochem.* 2006. **139**: 171–175.

9 Ryzhakov, G. and Randow, F., SINTBAD, a novel component of innate antiviral immunity, shares a TBK1-binding domain with NAP1 and TANK. *EMBO J.* 2007. **26**: 3180–3190.

10 Sasai, M., Oshiumi, H., Matsumoto, M., Inoue, N., Fujita, F., Nakanishi, M. and Seya, T., Cutting Edge: NF-kappaB-activating kinase-associated protein 1 participates in TLR3/Toll-IL-1 homology domain-containing adapter molecule-1-mediated IFN regulatory factor 3 activation. *J. Immunol.* 2005. **174**: 27–30.

11 Saito, T., Hirai, R., Loo, Y. M., Owen, D., Johnson, C. L., Sinha, S. C., Akira, S. *et al.*, Regulation of innate antiviral defenses through a shared repressor domain in RIG-I and LGP2. *Proc. Natl. Acad. Sci. USA* 2007. **104**: 582–587.

12 Hornung, V., Ellegast, J., Kim, S., Brzozka, K., Jung, A., Kato, H., Poeck, H. *et al.*, 5′-Triphosphate RNA is the ligand for RIG-I. *Science* 2006. **314**: 994–997.

13 Franca, R., Belfiore, A., Spadari, S. and Maga, G., Human DEAD-box ATPase DDX3 shows a relaxed nucleoside substrate specificity. *Proteins* 2007. **67**: 1128–1137.

14 Yedavalli, V. S., Neuveut, C., Chi, Y. H., Kleiman, L. and Jeang, K. T., Requirement of DDX3 DEAD box RNA helicase for HIV-1 Rev-RRE export function. *Cell* 2004. **119**: 381–392.

15 Kravchenko, V. V., Mathison, J. C., Schwamborn, K., Mercurio, F. and Ulevitch, R. J., IKKi/IKKepsilon plays a key role in integrating signals induced by pro-inflammatory stimuli. *J. Biol. Chem.* 2003. **278**: 26612–26619.

16 Soulat, D., Bürckstümmer, T., Westermayer, S., Goncalves, A., Bauch, A., Stefanovic, A., Hantschel, O. *et al.*, The DEAD-box helicase DDX3X is a critical component of the TANK-binding kinase 1-dependent innate immune response. *EMBO J.* 2008. **27**: 2135–2146.

17 Venkataraman, T., Valdes, M., Elsby, R., Kakuta, S., Caceres, G., Saijo, S., Iwakura, Y. *et al.*, Loss of DExD/H box RNA helicase LGP2 manifests disparate antiviral responses. *J. Immunol.* 2007. **178**: 6444–6455.

18 Schroder, M., Baran, M. and Bowie, A. G., Viral targeting of DEAD box protein 3 reveals its role in TBK1/IKKepsilon-mediated IRF activation. *EMBO J.* 2008. **27**: 2147–2157.

19 Gack, M. U., Shin, Y. C., Joo, C. H., Urano, T., Liang, C., Sun, L., Takeuchi, O. *et al.*, TRIM25 RING-finger E3 ubiquitin ligase is essential for RIG-I-mediated antiviral activity. *Nature* 2007. **446**: 916–920.

20 Oshiumi, H., Matsumoto, M., Hatakeyama, S. and Seya, T., Riplet/RNF135, a RING finger protein, ubiquitinates RIG-I to promote interferon-beta induction during the early phase of viral infection. *J. Biol. Chem.* 2009. **284**: 807–817.

21 Arimoto, K., Takahashi, H., Hishiki, T., Konishi, H., Fujita, T. and Shimotohno, K., Negative regulation of the RIG-I signaling by the ubiquitin ligase RNF125. *Proc. Natl. Acad. Sci. USA* 2007. **104**: 7500–7505.

22 Ariumi, Y., Kuroki, M., Abe, K., Dansako, H., Ikeda, M., Wakita, T. and Kato, N., DDX3 DEAD-box RNA helicase is required for hepatitis C virus RNA replication. *J. Virol.* 2007. **81**: 13922–13926.

23 **Chuang, R. Y., Weaver, P. L., Liu, Z. and Chang, T. H.,** Requirement of the DEAD-Box protein ded1p for messenger RNA translation. *Science* 1997. **275**: 1468–1471.

24 **Owsianka, A. M. and Patel, A. H.,** Hepatitis C virus core protein interacts with a human DEAD box protein DDX3. *Virology* 1999. **257**: 330–340.

25 **Mamiya, N. and Worman, H. J.,** Hepatitis C virus core protein binds to a DEAD box RNA helicase. *J. Biol. Chem.* 1999. **274**: 15751–15756.

26 **Sasai, M., Shingai, M., Funami, K., Yoneyama, M., Fujita, T., Matsumoto, M. and Seya, T.,** NAK-associated protein 1 participates in both the TLR3 and the cytoplasmic pathways in type I IFN induction. *J. Immunol.* 2006. **177**: 8676–8683.

27 **Oshiumi, H., Matsumoto, M., Funami, K., Akazawa, T. and Seya, T.,** TICAM-1, an adaptor molecule that participates in Toll-like receptor 3-mediated interferon-beta induction. *Nat. Immunol.* 2003. **4**: 161–167.

28 **Matsumoto, M., Funami, K., Tanabe, M., Oshiumi, H., Shingai, M., Seto, Y., Yamamoto, A. *et al.*,** Subcellular localization of Toll-like receptor 3 in human dendritic cells. *J. Immunol.* 2003. **171**: 3154–3162.

Abbreviations: **CARD:** caspase recruitment domain · **DEAD:** Asp-Glu-Ala-Asp · **DDX3:** DEAD/H BOX 3 · **IKKε:** I-kappa-B kinase ε · **IRF-3:** IFN regulatory factor-3 · **IP:** immunoprecipitation · **IPS-1:** IFN-β promoter stimulator-1 · **MDA5:** melanoma differentiation-associated gene 5 · **RIG-I:** retinoic acid inducible gene-I · **RLR:** RIG-I-like receptor · **TBK1:** TANK-binding kinase 1 · **VSV:** vesicular stomatitis virus

Full correspondence: Dr. Tsukasa Seya, Department of Microbiology and Immunology, Graduate School of Medicine, Hokkaido University, Kita-ku, Sapporo 060-8638, Japan
Fax: +81-11-706-7866
e-mail: seya-tu@pop.med.hokudai.ac.jp

See accompanying Commentary:
http://dx.doi.org/10.1002/eji.201040447

Received: 30/11/2009
Revised: 8/1/2010
Accepted: 19/1/2010
Accepted article online: 1/2/2010

Cancer Science
The official journal of the Japanese Cancer Association JCA

Adjuvant engineering for cancer immunotherapy: Development of a synthetic TLR2 ligand with increased cell adhesion

Takashi Akazawa,[1,2,5] Norimitsu Inoue,[1] Hiroaki Shime,[1,3] Ken Kodama,[4] Misako Matsumoto[2,3] and Tsukasa Seya[2,3]

Departments of [1]Molecular Genetics, [2]Immunology, Osaka Medical Center for Cancer and Cardiovascular Diseases, Osaka; [3]Department of Microbiology and Immunology, Hokkaido University Graduate School of Medicine, Sapporo; [4]Department of Surgery, Osaka Medical Center for Cancer and Cardiovascular Diseases, Osaka, Japan

(Recieved August 21, 2009/Revised December 8, 2009; March 23, 2010/Accepted March 28, 2010/Accepted manuscript online April 5, 2010/Article first published online May 7, 2010)

The development of effective immunoadjuvants for tumor immunotherapy is of fundamental importance. The use of *Mycobacterium bovis* bacillus Calmette-Guérin cell wall skeleton (BCG-CWS) in tumor immunotherapy has been examined in various clinical applications. Because BCG-CWS is a macromolecule that cannot be chemically synthesized, the development of an alternative synthetic molecule is necessary to ensure a constant supply of adjuvant. In the present study, a new adjuvant was designed based on the structure of macrophage-activating lipopeptide (MALP)-2, which is a Toll-like receptor (TLR)-2 ligand similar to BCG-CWS. Macrophage-activating lipopeptide-2, [S-(2,3-bispalmitoyloxypropyl)Cys (P2C) – GNNDESNISFKEK], originally identified in a Mycoplasma species, is a lipopeptide that can be chemically synthesized. A MALP-2 peptide was substituted with a functional motif, RGDS, creating a novel molecule named P2C-RGDS. RGDS was selected because its sequence constitutes an integrin-binding motif and various integrins are expressed in immune cells including dendritic cells (DCs). Thus, this motif adds functionality to the ligand. P2C-RGDS activated DCs and splenocytes more efficiently than MALP-2 over short incubation times *in vitro*, and the RGDS motif contributed to their activation. Furthermore, P2C-RGDS showed higher activity than MALP-2 in inducing migration of DCs to draining lymph node, and in inhibiting tumor growth *in vivo*. This process of designing and developing synthetic adjuvants has been named "adjuvant engineering," and the evaluation and improvement of P2C-RGDS constitutes a first step in the development of stronger synthetic adjuvants in the future. (*Cancer Sci* 2010; 101: 1596–1603)

Bacterial adjuvants that were used as biological response modifiers (BRM) for cancer immunotherapy in the 1970s have recently been re-evaluated.[1–3] Cancer antigens that had been identified in many laboratories were tested as peptide vaccines for clinical applications, but the peptides alone were not sufficient to fully activate the immune system.[4] These results suggested that the activation of the innate immune system, including dendritic cells (DCs), by a supporting adjuvant was important.[5–8] In peptide vaccine therapy, the T cells of the acquired immune system play an important role in recognizing and attacking tumor cells.[9] Dendritic cells play a key role in the regulation of the acquired immune system by presenting antigen and inducing a primary immune response. The identification of the Toll-like receptor (TLR) family advanced the understanding of DC function and of the role of adjuvants, because almost all microbial adjuvants work as TLR ligands and activate DCs.[10–12] These findings provide the basis for the understanding of the mechanism of adjuvant therapy.

Dr Azuma developed BCG-CWS, a cell-wall skeleton preparation of *Mycobacterium bovis* bacillus Calmette-Guérin,[13,14] as an antitumor immunotherapeutic adjuvant. Although many BRM studies have been discontinued, basic and clinical research on BCG-CWS has continued at Osaka Medical Center for Cancer. We reported that BCG-CWS is a ligand of TLR2/4[15–17] and acts as an effective adjuvant to induce CTLs in irradiated tumors in a mouse experimental model. These activities are mediated by the myeloid differentiation protein 88 (MyD88),[18] which is a TLR adaptor molecule. The effectiveness of BCG-CWS in improving the prognosis for cancer patients after surgery was confirmed through clinical research.[19]

Interleukin (IL)-23 and interferon (IFN)-γ are the main cytokines induced by BCG-CWS *in vivo*[14,19,20] and are important for antitumor immunity.[21,22] Interleukin-12 is well known as an antitumor cytokine,[23] and IL-23 shares the IL12p40 subunit with IL-12.[22] Unexpectedly, IL-23 advanced tumor growth in experiments with IL-23R$^{-/-}$ mice or neutralizing antibodies by interacting with Th17 cells.[24–26] However, systemic administration of IL-23 was also reported to have antitumor effects similar to those of IL-12,[27] and TLR2 ligands exhibit antitumor activity[28–30] that may be mediated by the induction of IL-23.

Although BCG-CWS is effective as an adjuvant, its clinical use is limited in purity, stability, and a stable supply because it cannot be chemically synthesized and is therefore prepared from bacterial cells. These factors indicate that there is a need to develop new synthetic adjuvants as effective as BCG-CWS. The present report describes the design of such adjuvants based on the structure of the TLR2 ligand and in consideration of the need for IL-23 induction. Macrophage-activating lipopeptide (MALP)-2, a lipopeptide of mycoplasmic origin, is a TLR2 ligand that can be chemically synthesized. No functional consensus peptide sequences were identified in MALP-2. The N-terminal cysteine of the 13-amino-acid peptide of bacterial origin was modified with 2 palmitates [Pam2Cys or P2C, S-(2,3-bispalmitoyloxypropyl)-cysteine],[31] but P2C alone does not work as a TLR2 ligand.[32] Bacterial and synthetic TLR2 ligands (MALP-2, FSL-1,[32] P2C-SKKKK[33]) contain mostly hydrophilic peptides, and the presence of solubilizers critically affects their TLR2 agonistic ability,[34] suggesting that the activity of compounds as TLR2 agonists correlates with their solubility.

CD11c is a member of the integrin superfamily and is known to be a marker of DCs.[35] Dendritic cells also express other integrin molecules such as αV/β3 and α5/β1, and the RGDS motif specifically binds to these integrins.[36,37] Virus particles expressing proteins containing the RGD motif efficiently infect DCs.[37] Therefore, a new TLR2 ligand was developed by

[5]To whom correspondence should be addressed.
E-mail: akazawa-ta@mc.pref.osaka.jp

doi: 10.1111/j.1349-7006.2010.01583.x

replacing the peptide of bacterial origin with a hydrophilic functional motif (adjuvant engineering). P2C and the RGDS peptide were linked to increase the efficiency of ligand adherence to DCs or other immune cells, and the effect of the new adjuvant on antitumor activities *in vitro* and *in vivo* was examined.

Materials and Methods

Mice, cells, and reagents. Toll/IL-1 receptor homology-containing adaptor molecule (TICAM)-$1^{-/-}$ mice were generated in our laboratory.[2] Toll-like receptor (TLR)-$2^{-/-}$ and MyD88$^{-/-}$ mice were provided by Shizuo Akira (Osaka University).[38] The mice were maintained under specific pathogen-free conditions in the animal facility of the Osaka Medical Center. They were backcrossed with C57BL/6 mice >8 times before use. Wild-type (WT) C57BL/6 mice were purchased from Japan Clea (Tokyo, Japan). All animal experiments were approved by the committee at Osaka Medical Center for Cancer. EG7 cells are ovalbumin-transfected EL4 and were obtained from the American Type Culture Collection (ATCC, Manassas, VA, USA).[39] B16D8 was established in our laboratory as a subline of the B16 melanoma cell line.[18] Cell lysates were prepared by the freeze-thaw method.

Preparation of mouse bone marrow-derived DCs (BMDCs), splenocytes, and lymph node cells. Bone marrow-derived DCs were prepared as previously described[35,40] with minor modifications, and were cultured in RPMI-1640 (Invitrogen, Carlsbad, CA, USA) containing 10 ng/mL mouse granulocyte-macrophage colony-stimulating factor (PeproTech EC, London, UK), 50 μM 2-mercaptoethanol (Invitrogen), 10 mM HEPES, and 10% FCS (Bio Whittaker, Walkersville, MD, USA). The inguinal lymph node cells and splenocytes were prepared by using Lympholyte-M (Cedarlane, Burlington, ON, Canada). CD11c-positive and -negative cells, and CD90-positive and -negative cells were separated from splenocytes by using CD11c or CD90 microbeads (Miltenyi Biotec, Auburn, CA, USA).

***In vitro* assay.** For the simple stimulation assay *in vitro*, BMDCs or splenocytes were cultured with 10 μg/mL of BCG-CWS,[18] 100 nM of MALP-2 and the designed lipopeptide (purity >90%; Biologica, Aichi, Japan) for 24 h (BMDCs, FACS), 48 h (BMDCs, ELISA), or 72 h (splenocytes, ELISA). For the inhibition assay, BMDCs or splenocytes were pre-incubated with the indicated concentrations of RGDS peptide or anti-CD29 antibody (eBioscience, San Diego, CA, USA) at 4°C for 30 min before stimulating them with TLR2 ligands at 4°C for 60 min. The cells were then washed and re-cultured for 48 h (BMDCs, ELISA) or 72 h (splenocytes, ELISA). The Mixed Lymphocyte Reaction (MLR) assay was performed as previously described,[40] and the results were analyzed as uptake of [^{3}H]thymidine (1 μCi/well; Amersham Biosciences, Piscataway, NJ, USA). Bone marrow-derived DCs stimulated with TLR2 ligands for 24 h (C57BL/6, 5×10^4 cells) were co-cultured with CD90-positive T cells (BALB/c, 10^5 cells) for 72 h. To exclude the possible effect of contaminating lipopolysaccharide, lipopeptides were pretreated with polymyxin B (Sigma-Aldrich, St. Louis, MO, USA) at 37°C for 60 min.

Fluorescence-activated cell sorter (FACS) analysis, intracellular cytokine staining, and ELISA. For FACS analysis, cells were suspended in PBS containing 0.1% sodium azide and 1% FCS, and then incubated for 30 min at 4°C with FITC-conjugated antimouse CD80, antimouse CD86, antimouse CD8, or isotype control antibody; or with phycoerythrin-conjugated antimouse CD4 or isotype control antibody (eBioscience). The cells were washed, and their fluorescence intensities were measured by FACS analysis. For intracellular cytokine staining, splenocytes were stimulated with P2C-RGDS for 72 h and Brefeldin A (GolgiPlug; BD Biosciences, San Diego, CA, USA) for the last 6 h. Cells were stained with phycoerythrin-conjugated antimouse CD3e, antimouse CD4, antimouse CD8a antibodies, allophycocyanin-conjugated antimouse CD11c, or antimouse NK1.1 antibodies (eBioscience), followed by fixation and permeabilization with the Cytofix/Cytoperm plus Kit (BD Biosciences). Cells were stained intracellularly with FITC-labeled anti-IFN-γ antibody (XMG1.2; eBioscience). For ELISA, samples were stored at –80°C and analyzed with ELISA kits for IFN-γ, TNF-α, and IL12p40 (Biosource, Camarillo, CA, USA).

***In vivo* therapy model.** C57BL/6 mice were shaved on the back and injected subcutaneously with 200 μL of $1–2 \times 10^6$ syngeneic EG7 cells in PBS on Day 0. Thereafter, the treatment was performed three times, on Days 16, 20, and 23, and tumor volumes were measured using a caliper every 2–3 days. A volume of 50 μL of a mixture consisting of 10 nmol of lipopeptide and the cell lysate of 2×10^5 EG7 cells with or without 10 nmol of RGDS peptide was injected intradermally around the transplanted tumor. Tumor volume was calculated using the formula: Tumor volume (cm^3) = (long diameter) × (short diameter) × (short diameter) × 0.4. Statistical analysis was performed with the Student's *t*-test.

***Ex vivo* assay.** C57BL/6 mice were treated intradermally with a mixture of 10 nmol of lipopeptide and the cell lysate of 2×10^5 EG7 cells every 3 days for >4 treatments. At 24 h after the last treatment, the mice were sacrificed by etherization, and then the splenocytes and lymph node cells were prepared and cultured for 4 days to be primed by DCs and macrophages. The cytolytic activities of lymph node cells were then analyzed with a ^{51}Cr release assay.[18] The percentage of specific lysis was calculated using the formula: %Specific lysis = [(experimental release – spontaneous release)/(total release – spontaneous release)] × 100. The proportions of CD8- and CD11c-positive cells in the lymph nodes or spleen were analyzed by FACS.

Results

To design a new TLR2 ligand with activity equivalent to that of BCG-CWS, the minimum lipopeptide unit, P2C, was connected to the RGDS integrin-binding motif to increase adherence to DCs, forming P2C-RGDS (Fig. 1a). The hydrophobicity and pI of P2C-RGDS were similar to those of MALP-2, and the molecular weight of P2C-RGDS was half that of MALP-2 (Fig. 1b).

First, the synthetic adjuvants were tested for their capacity to activate BMDCs *in vitro* when these compounds were added to the culture medium. P2C-RGDS enhanced the expression of CD80 and CD86 in BMDCs at a level equal to that of MALP-2, the positive control (Fig. 2a). P2C-RGDS also enhanced the production of IL12p40 and TNF-α (Fig. 2b) and the proliferation of allogeneic T cells co-cultured with the BMDCs. Thus, P2C-RGDS and MALP-2 stimulate DCs equally *in vitro*, whereas P2C does not show the same activity.

Macrophage-activating lipopeptide-2 is a ligand of TLR2/6 that activates DCs through MyD88. To examine the TLR2 and TLR signaling pathway-dependence of P2C-RGDS, BMDCs were prepared from TLR2$^{-/-}$, MyD88$^{-/-}$, or TICAM-$1^{-/-}$ mice and stimulated with these synthetic lipopeptides. Both MALP-2 and P2C-RGDS enhanced the expression of CD80 and CD86 in BMDCs derived from WT or TICAM-$1^{-/-}$ mice, but not TLR2$^{-/-}$ or MyD88$^{-/-}$ mice (Fig. 3), suggesting that P2C-RGDS is a TLR2 ligand with activity similar to that of MALP-2 *in vitro*.

Next, the functional dependence of P2C-RGDS as a TLR2 ligand on not only its hydrophilicity, but also on the motif-specificity of the peptide sequences, was tested. Since MALP2 and P2C-RGDS activated DCs to the same extent at 37°C for 48 h, DCs were instead stimulated at 4°C for 1 h, then washed and re-cultured at 37°C for 48 h. Under these conditions, P2C-RGDS induced IL12p40 more efficiently than MALP-2 (Fig. 4a). To analyze the specificity of the RGDS peptide,

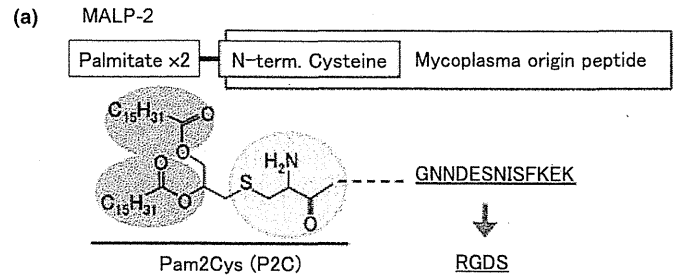

(b)

Compounds		M.W.	Peptide	pI	Hydrophobicity
P2C		672.5	P2 C	—	—
MALP-2	(N)	2134.1	P2 C G N N D E S N I S F K E K	*4.68	−1.5
FSL-1	(N)	1666.1	P2 C G D P K H P K S F	8.21	−1.36
P2C-SKKKK	(S)	1271.8	P2 C S K K K K	10.04	−2.32
P2C-RGDS	(S)	1087.5	P2 C R G D S	*5.83	−1.34

Fig. 1. The structure of the adjuvant developed in the present study, a synthetic Toll-like receptor (TLR)-2 ligand containing the RGDS motif. (a) The structure of macrophage-activating lipopeptide (MALP)-2. The N-terminal cysteine of a peptide derived from a mycobacterium is modified with 2 palmitates [Pam2Cys, P2C, S-(2,3-bispalmitoyloxypropyl)cysteine]. RGDS was conjugated to P2C to form P2C-RGDS because of its hydrophilicity and its additional function as an integrin-binding motif for cell adhesion. (b) The structure, molecular weight, isoelectric point (pI), and hydrophobicity of synthetic (P2C-RGDS, P2C-SKKKK) and natural (MALP-2, FSL-1) lipopeptides used in this study. The pI and hydrophobicity of the peptide were calculated using ProtParam tools (http://br.expasy.org/tools/protparam.html). The pI and hydrophobicity of P2C-RGDS were almost equivalent to those of MALP-2. The molecular weight of P2C-RGDS was about half that of MALP-2. N, natural TLR2 ligand; S, synthetic TLR2 ligand. The asterisks (*) indicate acidic peptides. The gray boxes indicate hydrophobic amino acids.

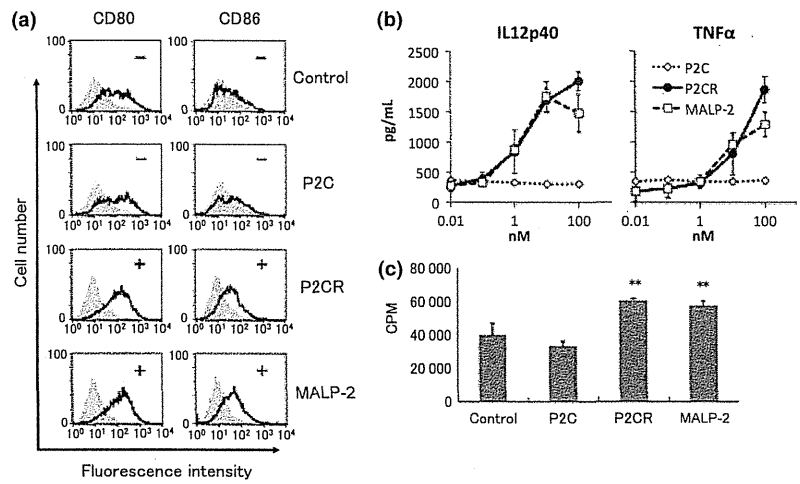

Fig. 2. P2C-RGDS activates bone marrow-derived dendritic cells (BMDCs) as much as macrophage-activating lipopeptide (MALP)-2 *in vitro*. (a) The enhancement of CD80/CD86 expression of BMDCs stimulated with the indicated compounds (100 nM) for 24 h was observed by FACS analysis. (b) Interleukin (IL)12p40 and tumor necrosis factor (TNF)-α production in BMDCs stimulated with each compound for 48 h was determined by ELISA. (c) The proliferation of allogeneic T cells co-cultured with activated-BMDCs for 72 h was measured by the [^{3}H] thymidine uptake method. Bone marrow-derived dendritic cells were treated with each compound for 24 h before co-culture with T cells. CPM, count per minute. $^{**}P < 0.01$ *vs* control (Student's *t*-test). P2CR, P2C-RGDS.

IL12p40 production was inhibited by the addition of an RGDS competitor peptide or anti-integrin β1 antibody to the assay. The addition of the RGDS competitor peptide and the integrin blocking antibodies partially attenuated the production of IL12p40 induced by P2C-RGDS, but not that induced by MALP-2 (Fig. 4b,c). These results indicate that not only hydrophilicity but also the functional RGDS motif contributes to the activation of DCs *in vitro* at short incubation times.

The P2C-RGDS-induced production of IFN-γ was evaluated next, using *in vitro* whole splenocyte stimulation. The activities of P2C-RGDS and MALP-2, as measured by IFN-γ production, were comparable and weaker than that of BCG-CWS when splenocytes were simply stimulated with each compound for 72 h (Fig. 5a). However, when splenocytes were stimulated with each compound at 4°C for 1 h and re-cultured at 37°C for 72 h, the P2C-RGDS-induced production of IFN-γ was stronger than that induced by MALP-2 and it was attenuated mostly by the RGDS peptide. Furthermore, the splenocytes stimulated with P2C-RGDS produced as much IFN-γ as those stimulated with BCG-CWS at 4°C for 1 h (Fig. 5b). Interferon-γ production was not detected in splenocytes depleted of CD11c-positive dendritic cells, and IFN-γ production could be restored under these conditions by adding back CD11c-positive cells. These data indicate that IFN-γ production by splenocytes following stimulation with

doi: 10.1111/j.1349-7006.2010.01583.x

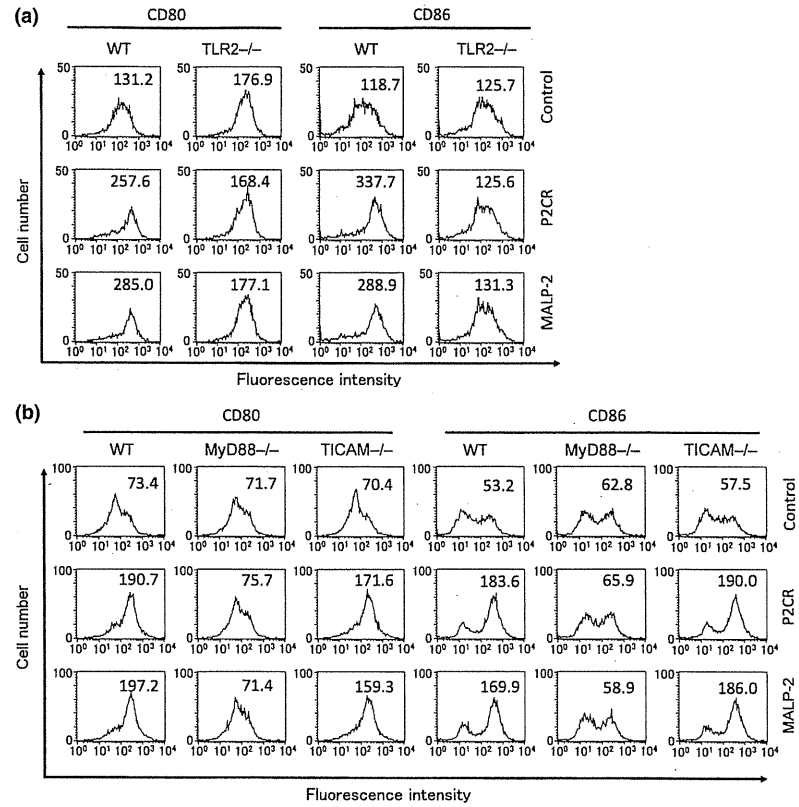

Fig. 3. P2C-RGDS activates bone marrow-derived dendritic cells (BMDCs) in a Toll-like receptor (TLR)-2 and myeloid differentiation protein (MyD)-88-dependent manner *in vitro*. (a,b) Bone marrow-derived dendritic cells were prepared from mice lacking TLR2 (TLR2$^{-/-}$) and TLR adaptor molecules (MyD88$^{-/-}$ and TICAM-1$^{-/-}$). CD80 and CD86 expression was observed by FACS analysis at 24 h after BMDCs were stimulated with MALP-2 or P2C-RGDS. The numbers in the panels represent mean fluorescence intensities. P2C-RGDS and MALP-2 activated BMDCs via TLR2 and MyD88, but not via the Toll/IL-1 receptor homology-containing adaptor molecule (TICAM)-1 pathway. P2CR, P2C-RGDS.

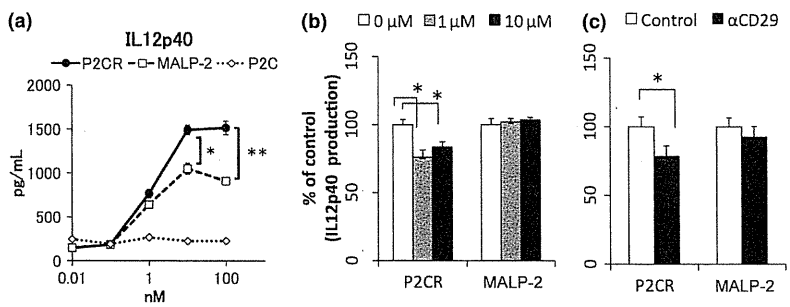

Fig. 4. P2C-RGDS efficiently activates bone marrow-derived dendritic cells (BMDCs) in an RGDS motif–dependent manner *in vitro* over short incubation times. (a) Interleukin (IL)12p40 production of BMDCs stimulated with each Toll-like receptor (TLR)-2 ligand at 4°C for 1 h. Bone marrow-derived dendritic cells were washed after the stimulation and re-cultured for 48 h. Interleukin12p40 production was determined by ELISA. (b) Bone marrow-derived dendritic cells were pretreated with the indicated concentrations of RGDS peptide (P2C-modification free) as a competitor at 4°C for 30 min. Then, the BMDCs were stimulated with TLR2 ligands (10 nM) at 4°C for 1 h. Interleukin12p40 production by BMDCs was determined by ELISA. Data are shown as percentages of each control value. (c) The inhibition effects of α-CD29 (integrin β1) antibody on IL12p40 production of BMDCs. Bone marrow-derived dendritic cells were pre-treated with 10 μg/mL of each antibody at 4°C for 30 min before stimulation. P2CR, P2C-RGDS.

P2C-RGDS was mediated by DC activation (Fig. 5c). IFN-γ production was also impaired by depletion of CD90 (Thy1)-positive T cells (Fig. 5c). Further assessment of IFN-γ producing cells by intracellular cytokine staining revealed that IFN-γ was mainly detected in CD3- or CD8-positive cells, and in CD4-, NK1.1-, or CD11c-negative cells stimulated with P2C-RGDS (Fig. 5d).

Finally, the antitumor activity of P2C-RGDS *in vivo* was investigated using a tumor-implantation model. The mice were transplanted with EG7 on day 0, and treated with synthetic lipopeptide (10 nmol) and the cell lysate of EG7 cells (2×10^5) on Days 16, 20, and 23. The minimum lipopeptide unit P2C showed no *in vivo* antitumor activity similar to the activation of DCs *in vitro*. Although MALP-2-treated mice showed a slightly smaller tumor volume than control mice, this difference was not significant. However, P2C-RGDS showed a significant antitumor effect (Student's *t*-test, $P < 0.05$ *vs* control; Fig. 6a). Moreover, the mixture of P2C and the RGDS peptide showed no antitumor activity (Fig. 6b). Next, lymph node cells from mice immunized with EG7 lysate and P2C-RGDS or MALP-2 were isolated, and the cytotoxicity against EG7 and B16D8 cells was measured using a ^{51}Cr release assay. P2C-RGDS specifically

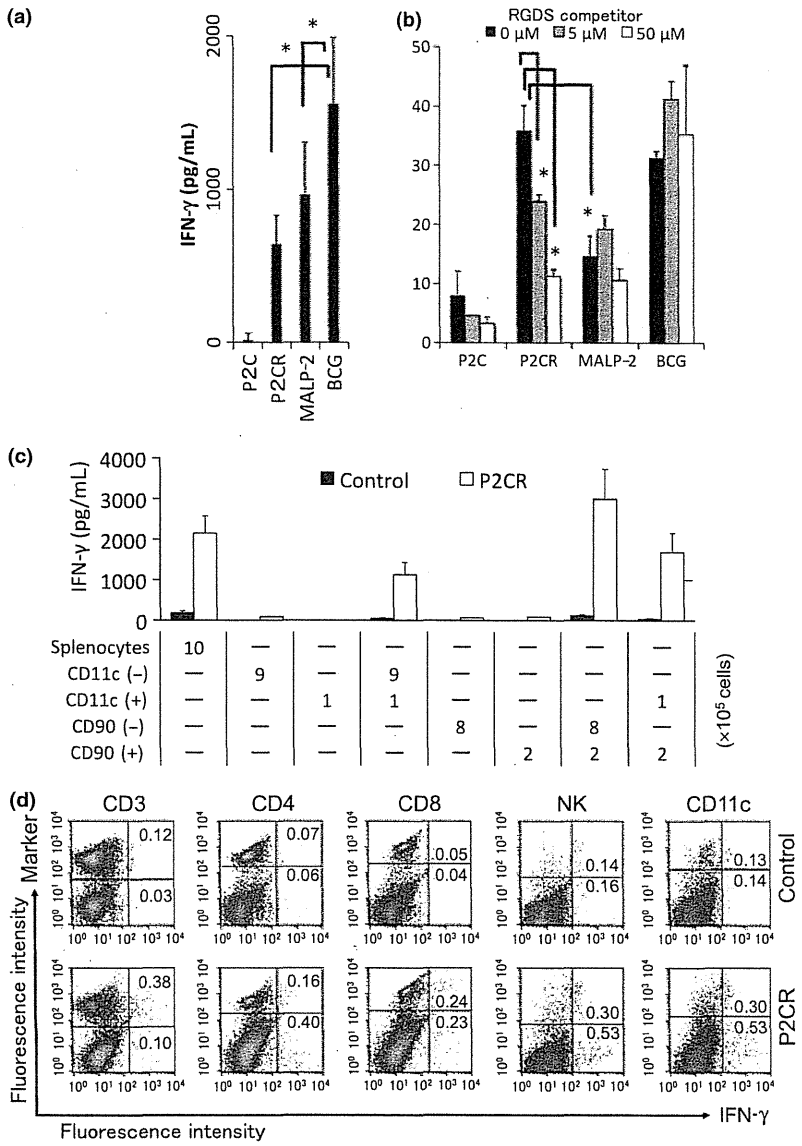

Fig. 5. P2C-RGDS efficiently activates splenocytes in an RGDS motif-dependent manner. (a) Interferon (IFN)-γ production by splenocytes stimulated with each compound for 72 h. (b) The effect of RGDS competitor peptide pretreatment on IFN-γ production. The RGDS competitor attenuated IFN-γ production from splenocytes stimulated with P2C-RGDS at 4°C for 1 h. (c) The roles of CD11c-positive cells (dendritic cells) and CD90-positive cells (T cells) on IFN-γ production by splenocytes. The splenocytes were separated into $CD11c^+$ and $CD11c^-$ cells, or $CD90^+$ and $CD90^-$ cells by using MACS beads. Cells were prepared based on the recovery ratio and stimulated with P2C-RGDS for 72 h. $*P < 0.05$, $**P < 0.01$ (Student's *t*-test); n.d, not detected. (d) Intracellular IFN-γ staining of splenocytes with various expression markers. Density plots show the expression of each surface marker and intracellular staining for IFN-γ, and the numbers indicate the proportion of IFN-γ-positive cells (%). P2CR, P2C-RGDS.

induced a stronger cytotoxic activity against EG7 than MALP-2, but the lymph node cells were not sufficiently cytotoxic against the negative target B16D8 cells (Fig. 6c). In addition, lymph node cells were cultured continuously with live EG7 cells for 96 h and the proportion of CD8-positive cells was analyzed by FACS. CD8-positive cells in lymph nodes derived from P2C-RGDS-treated mice remained at a level of approximately 16% of total cells, but most CD8-positive cells from MALP-2-treated mice were lost after culture with EG7 (Fig. 6d). The proportion of CD8-positive cells in a splenocyte population derived from immunized mice was also evaluated using FACS analysis. CD8-positive cells were proportionally higher among splenocytes derived from mice treated with P2C-RGDS than among splenocytes derived from mice treated with MALP-2 (Fig. 6e). Necrosis was observed on the surface of tumors after P2C-RGDS but not after MALP-2 treatment, and CD8-positive cells were detected around the necrosis tissue by immunostaining (data not shown). These data suggest that P2C-RGDS induces and activates CTLs more efficiently than MALP-2. Moreover, to analyze the mechanism underlying the strong antitumor effect of P2C-RGDS *in vivo*, the proportions of CD11c-positive cells in draining lymph nodes were analyzed in mice treated with MALP-2 or P2C-RGDS for 24 h. P2C-RGDS induced the migration of CD11c-positive cells to the draining lymph nodes more effectively than MALP2 ($P = 0.055$, Fig. 6f).

Discussion

Natural TLR2 ligands of bacterial origin, such as MALP-2[31,41,42] and FSL-1,[32] have been reported to effectively activate CD8-positive T cells and induce antitumor activity. Because these lipopeptides are hydrophilic, it was predicted that the hydrophilicity of the peptide might be important for its activity.[31–34] Several researchers have relied on a chemobiologic strategy of producing amino acid replacements to explore which portion of the lipopeptide sequence possesses effective adjuvant activity.[43] Using this strategy, Takeda developed Tan-1511 analogues that show high levels of activity in the induction of granulopoiesis.[43] Another strategy has been to randomly search for sequences or peptides effective at enhancing TLR2 ligand

doi: 10.1111/j.1349-7006.2010.01583.x

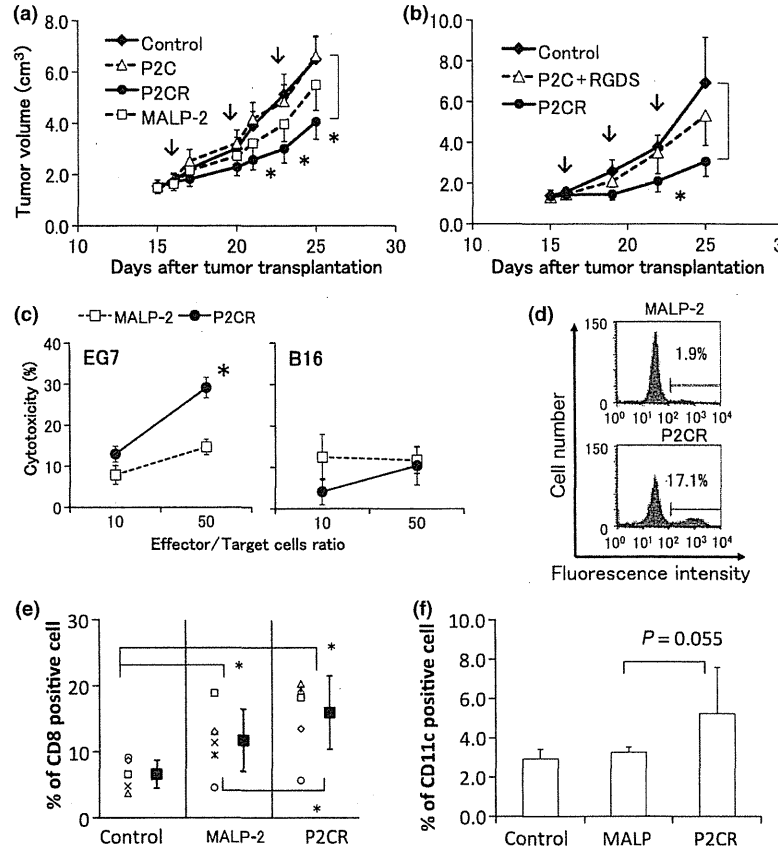

Fig. 6. P2C-RGDS is more effective at retarding tumor growth and inducing CD8-positive cells than macrophage-activating lipopeptide (MALP)-2 *in vivo* and *ex vivo*. Antitumor effect of P2C-RGDS and MALP-2 (a), and of a mixture of P2C and RGDS peptide (b), in the EG7-implanted mouse model (C57BL6-EG7 model). Mice were treated with Toll-like receptor (TLR)-2 ligand and EG7 lysate on Days 16, 20, and 23 (arrows). The data are shown as means ± SE ($n = 9$). $^*P < 0.05$ *vs* control (Student's *t*-test). (c) Lymph node cells derived from P2C-RGDS and EG7 lysate-immunized mice showed stronger cytotoxicity than cells from MALP-2-immunized mice against EG7 but not B16 (^{51}Cr release assay). $^*P < 0.05$ *vs* MALP-2 (Student's *t*-test). (d) CD8-positive T cells were more effectively induced in lymph nodes derived from mice immunized with P2C-RGDS and EG7 lysate than in those immunized with MALP-2. The lymph node cells in Figure 6(c) were cultured with live EG7 for 96 h, and then the proportion of CD8-positive T cells was analyzed. (e) Immunization with P2C-RGDS and EG7 lysate induced CD8-positive T cells in splenocytes more efficiently than immunization with MALP-2. The proportions of CD8-positive cells in splenocytes were determined by FACS analysis at 96 h after the initiation of splenocyte cultivation. Each symbol indicates an individual experiment. The closed squares represent average ± SD. $^*P < 0.05$ (paired *t*-test). (f) The proportion of CD11c-positive cells in the draining lymph nodes at 24 h after immunization. CD11c-positive cells were examined by FACS analysis. $P = 0.055$ *vs* MALP-2 (Student's *t*-test). P2CR, P2C-RGDS.

activity.[44] The purpose of the current project was to design a TLR2 ligand with an additional function through the addition of a hydrophilic, functional peptide that could be developed as a new synthetic adjuvant (Fig. 1). In comparison to a prior developmental strategies, the present design has the advantage of allowing the selection of various functions, and because the designed lipopeptides do not exist in nature, they could show new or enhanced properties. In the present study, the TLR2 ligand was designed to possess stronger adhesive capacity through the linking of the RGDS peptide to P2C.

The compound P2C-RGDS was developed and shown to be as effective as MALP-2 in generating BMDC responses *in vitro*, such as the enhancement of a maturation marker (CD80 and CD86) and cytokine induction when DCs were cultured with each compound for 24–48 h (Fig. 2). P2C-RGDS and MALP-2 also activated DCs through the TLR2–MyD88 pathway (Fig. 3),[38] but P2C-RGDS activated DCs more efficiently than MALP2, and the RGDS integrin binding motif was found to be important for DCs activation over short incubation times (Fig. 4). Because DCs were treated with compounds for only 1 h, then washed and re-cultured at 37°C for 48 h in these experiments, it was predicted that P2C-RGDS might efficiently adhere to the DCs in short incubation times, and then stimulate DCs continuously at the surface or in the phagosome of DCs. Whole splenocytes stimulated with P2C-RGDS also produced more IFN-γ than MALP-2 over short incubation times (Fig. 5b), and the production of IFN-γ by splenocytes depended on CD11c-positive DCs (Fig. 5c). These data suggest that the adhesion properties of P2C-RGDS caused the efficient activation of DCs, and reflected splenocyte activation. The stronger IFN-γ induction by P2C-RGDS might also be due to its retention in the culture system by adherence to various cells among the splenocytes. Moreover, P2C-RGDS may be retained in local regions for a long time via integrin binding *in vivo*, leading to the efficient activation of immune cells such as dermal DCs. P2C-RGDS induced the migration of CD11c-positive cells into the draining lymph nodes more effectively than MALP-2 in *in vivo* experiments (Fig. 6f). These DCs might activate CD8-positive cells, enhance cytotoxicity (Fig. 6c), and lead to retardation of tumor growth (Fig. 6a). These data suggest that the greater activation of DCs by P2C-RGDS compared to MALP2 influences IFN-γ production by splenocytes, thereby resulting in increased cytotoxicity and antitumor effects *in vivo*.

The induction of IFN-γ production by BCG-CWS treatment is one of the indexes for continuing treatment in clinical applications,[14,19] and the response can be confirmed in mouse experiments. Interferon-γ stimulation up-regulates the expression of MHC class I in tumor cells,[45] presumably improving tumor recognition by immune cells, and leading to increased suppression of tumor growth. With short stimulation periods, P2C-RGDS induced as much IFN-γ as BCG-CWS. Although the present compound was designed without considering IFN-γ induction, results show that CD8-positive cells produced IFN-γ in splenocytes stimulated with P2C-RGDS alone in the absence of antigen peptide (Fig. 5). The mechanism of IFN-γ induction by P2C-RGDS should be analyzed in the future. The tumor volume of the BCG-CWS treatment group was about 60% of that of the control on Day 22 (data not shown), and the therapeutic effects of P2C-RGDS were almost equivalent to those of BCG-CWS. Because BCG-CWS must be emulsified with drakeol, the use of P2C-RGDS has significant advantages.

The integrin binding sequence has served as the basis for the design of drugs that depend on adhesive activity. In the present work, this adhesive function was applied to TLR ligands to enhance immunoadjuvant activity. Cilengitide, a cyclic RGD peptide, was developed as an integrin αV antagonist, which impairs angiogenesis, tumor growth, and metastasis[46] because integrins are expressed on various tumor cells.[47] Although EG7 expresses integrin αV, β1, and β3, P2C-RGDS and RGDS peptide did not show direct cytotoxic activity against EG7 cells at concentrations up to 100 nM (data not shown). Furthermore, the adjuvant activities of P2C-RGDS were compared to those of a mixture of P2C and RGDS peptide. P2C had no adjuvant activity, such as the activation of DCs and splenocytes *in vitro* or antitumor effect *in vivo* by lipopeptides (Figs 2b, 5a, 6a). The mixture did not show any effects *in vivo* such as appreciable antitumor activity (Fig. 6b). Based on these results, the stronger antitumor activity of P2C-RGDS compared to that of MALP-2 is thought to occur through an increase in cell adhesive ability, but not through the inhibition of angiogenesis.

Concerning the relationship between TLR and its ligand, it is suggested that a co-receptor plays a key role for TLR binding and signaling[1,7,48] as observed previously for CD14 in the Lipopolysaccharide (LPS)–TLR4 signaling pathway. Although integrin binding is predicted to support the capture and phagocytosis of ligands by DCs, integrin signaling in addition to TLR signaling might influence adjuvant activity. Stronger adjuvants will be developed by selecting for other properties, in addition to TLR signaling, that are essential for adjuvant activity, and the integrin signal could be one of the candidates.

In the present work, the inclusion of an integrin-binding motif in a TLR2 ligand was examined for its effect in increasing the activity of the compound as an antitumor adjuvant by enhancing adhesion of the ligand to DCs and other cells. Dendritic cells efficiently recognized P2C-RGDS, which they adhered to and maintained around cells, and P2C-RGDS showed stronger antitumor activity than MALP-2 *in vivo*. The present adjuvant-engineering project is a new strategy to incorporate biological findings into drug design. Targeting peptides are used to elicit a strictly selective response among immune cells. A targeted strategy can effectively activate immune cells at a low concentration while not affecting other cells whose activation might lead to side effects. More than 20 TLR2 ligands with 10 alternative functions have already been synthesized by adjuvant engineering and our group is working to develop the strongest adjuvant through continued evaluation and improvements.

Acknowledgments

This work was supported in part by KAKENHI (15790069; 19790301; 20200075; 21790400) from the Ministry of Education, Culture, Science, and Technology of Japan; The Uehara Memorial Foundation; Osaka Community Foundation; and The Charitable Trust Osaka Cancer Researcher Fund. We are grateful to Drs K. Toyoshima, H. Koyama, S. Imaoka, S. Hori, K. Kato, and M. Tatsuta (Osaka Medical Center for Cancer, Osaka) for their support of this work. We are grateful to Dr K. Kikuchi (Sapporo Medical University, Sapporo), who gave the name "adjuvant engineering" to our project. Thanks are also due to N. Kanto, and T. Yasuda, E. Takahara, Y. Mimura, and M. Yabu (Osaka Medical Center for Cancer, Osaka) for their assistance.

References

1 Seya T, Akazawa T, Tsujita T, Matsumoto M. Role of Toll-like receptors in adjuvant-augmented immune therapies. *Evid Based Complement Alternat Med* 2006; **3**(1): 31–8.
2 Akazawa T, Ebihara T, Okuno M *et al.* Antitumor NK activation induced by the Toll-like receptor 3-TICAM-1 (TRIF) pathway in myeloid dendritic cells. *Proc Natl Acad Sci U S A* 2007; **104**(1): 252–7.
3 Okamoto M, Oshikawa T, Tano T *et al.* Involvement of Toll-like receptor 4 signaling in interferon-g production and antitumor effect by streptococcal agent OK-432. *J Natl Cancer Inst* 2003; **95**(4): 316–26.
4 Rosenberg SA, Yang JC, Restifo NP. Cancer immunotherapy: moving beyond current vaccines. *Nat Med* 2004; **10**(9): 909–15.
5 Celis E. Toll-like receptor ligands energize peptide vaccines through multiple paths. *Cancer Res* 2007; **67**(17): 7945–7.
6 Kanzler H, Barrat FJ, Hessel EM, Coffman RL. Therapeutic targeting of innate immunity with Toll-like receptor agonists and antagonists. *Nat Med* 2007; **13**(5): 552–9.
7 Seya T, Akazawa T, Uehori J, Matsumoto M, Azuma I, Toyoshima K. Role of toll-like receptors and their adaptors in adjuvant immunotherapy for cancer. *Anticancer Res* 2003; **23**(6a): 4369–76.
8 Akira S, Uematsu S, Takeuchi O. Pathogen recognition and innate immunity. *Cell* 2006; **124**: 783–801.
9 Miconnet I, Coste I, Beermann F *et al.* Cancer vaccine design: a novel bacterial adjuvant for peptide-specific CTL induction. *J Immunol* 2001; **166**(7): 4612–19.
10 Iwasaki A, Medzhitov R. Toll-like receptor control of the adaptive immune responses. *Nat Immunol* 2004; **5**: 987–95.
11 Kaisho T, Akira S. Toll-like receptors as adjuvant receptors. *Biochim Biophys Acta* 2002; **1589**(1): 1–13.
12 Hemmi H, Takeuchi O, Kawai T *et al.* A Toll-like receptor recognizes bacterial DNA. *Nature* 2000; **408**(6813): 740–5.
13 Azuma I, Ribi EE, Meyer TJ, Zbar B. Biologically active components from mycobacterial cell walls: I Isolation and composition of cell wall skeleton and component P3. *J Natl Cancer Inst* 1974; **52**: 95–101.
14 Hayashi A, Doi O, Azuma I, Toyoshima K. Immuno-friendly use of BCG-cell wall skeleton remarkably improves the survival rate of various cancer patients. *Proc Jpn Acad* 1998; **74** Ser. B: 50–5.
15 Uehori J, Fukase K, Akazawa T *et al.* Dendritic cell maturation induced by muramyl dipeptide (MDP) derivatives: monoacylated MDP confers TLR2/TLR4 activation. *J Immunol* 2005; **174**(11): 7096–103.
16 Tsuji S, Matsumoto M, Takeuchi O *et al.* Maturation of human dendritic cells by cell wall skeleton of Mycobacterium bovis bacillus Calmette-Guérin: involvement of toll-like receptors. *Infect Immun* 2000; **68**: 6883–90.
17 Uehori J, Matsumoto M, Tsuji S *et al.* Simultaneous blocking of human Toll-like receptor 2 and 4 suppresses myeloid dendritic cell activation induced by Mycobacterium bovis bacillus Calmette-Guérin (BCG)-peptidoglycan (PGN). *Infect Immun* 2003; **71**: 4238–49.
18 Akazawa T, Masuda H, Saeki Y *et al.* Adjuvant-mediated tumor regression and tumor-specific cytotoxic response are impaired in MyD88-deficient mice. *Cancer Res* 2004; **64**(2): 757–64.
19 Kodama K, Higashiyama M, Takami K *et al.* Innate immune therapy with a Bacillus Calmette-Guérin cell wall skeleton after radical surgery for non-small cell lung cancer: a case-control study. *Surg Today* 2009; **39**(3): 194–200.
20 Begum NA, Ishii K, Kurita-Taniguchi M *et al.* Mycobacterium bovis BCG cell wall-specific differentially expressed genes identified by differential display and cDNA subtraction in human macrophages. *Infect Immun* 2004; **72**(2): 937–48.
21 Matsumoto M, Seya T, Kikkawa S *et al.* Interferon gamma-producing ability in blood lymphocytes of patients with lung cancer through activation of the innate immune system by BCG cell wall skeleton. *Int Immunopharmacol* 2001; **1**(8): 1559–69.
22 Oppmann B, Lesley R, Blom B *et al.* Novel p19 protein engages IL-12p40 to form a cytokine, IL-23, with biological activities similar as well as distinct from IL-12. *Immunity* 2000; **13**(5): 715–25.
23 Zou JP, Yamamoto N, Fujii T *et al.* Systemic administration of rIL-12 induces complete tumor regression and protective immunity: response is correlated with a striking reversal of suppressed IFN-g production by anti-tumor T cells. *Int Immunol* 1995; **7**(7): 1135–45.
24 Langowski JL, Zhang X, Wu L *et al.* IL-23 promotes tumour incidence and growth. *Nature* 2006; **442**(7101): 461–5.
25 Kolls JK, Lindén A. Interleukin-17 family members and inflammation. *Immunity* 2004; **21**(4): 467–76.
26 Shime H, Yabu M, Akazawa T *et al.* Tumor-secreted lactic acid promotes IL-23/IL-17 proinflammatory pathway. *J Immunol* 2008; **180**(11): 7175–83.
27 Kaiga T, Sato M, Kaneda H, Iwakura Y, Takayama T, Tahara H. Systemic administration of IL-23 induces potent antitumor immunity primarily mediated through Th1-type response in association with the endogenously expressed IL-12. *J Immunol* 2007; **178**(12): 7571–80.
28 Jackson DC, Lau YF, Le T *et al.* A totally synthetic vaccine of generic structure that targets Toll-like receptor 2 on dendritic cells and promotes

doi: 10.1111/j.1349-7006.2010.01583.x

antibody or cytotoxic T cell responses. *Proc Natl Acad Sci U S A* 2004; **101**(43): 15440–5.
29 Schneider C, Schmidt T, Ziske C *et al.* Tumour suppression induced by the macrophage activating lipopeptide MALP-2 in an ultrasound guided pancreatic carcinoma mouse model. *Gut* 2004; **53**(3): 355–61.
30 Murata M. Activation of Toll-like receptor 2 by a novel preparation of cell wall skeleton from Mycobacterium bovis BCG Tokyo (SMP-105) sufficiently enhances immune responses against tumors. *Cancer Sci* 2008; **99**(7): 1435–40.
31 Mühlradt PF, Kiess M, Meyer H, Süssmuth R, Jung G. Isolation, structure elucidation, and synthesis of a macrophage stimulatory lipopeptide from Mycoplasma fermentans acting at picomolar concentration. *J Exp Med* 1997; **185**(11): 1951–8.
32 Okusawa T, Fujita M, Nakamura J *et al.* Relationship between structures and biological activities of mycoplasmal diacylated lipopeptides and their recognition by toll-like receptors 2 and 6. *Infect Immun* 2004; **72**(3): 1657–65.
33 Omueti KO, Beyer JM, Johnson CM, Lyle EA, Tapping RI. Domain exchange between human toll-like receptors 1 and 6 reveals a region required for lipopeptide discrimination. *J Biol Chem* 2005; **280**(44): 36616–25.
34 Voss S, Ulmer AJ, Jung G, Wiesmüller KH, Brock R. The activity of lipopeptide TLR2 agonists critically depends on the presence of solubilizers. *Eur J Immunol* 2007; **37**(12): 3489–98.
35 Inaba K, Pack M, Inaba M, Sakuta H, Isdell F, Steinman RM. High levels of a major histocompatibility complex II-self peptide complex on dendritic cells from the T cell areas of lymph nodes. *J Exp Med* 1997; **186**: 665–72.
36 Harui A, Roth MD, Vira D, Sanghvi M, Mizuguchi H, Basak SK. Adenoviral-encoded antigens are presented efficiently by a subset of dendritic cells expressing high levels of aV-b3 integrins. *J Leukoc Biol* 2006; **79**(6): 1271–8.
37 Okada N, Masunaga Y, Okada Y *et al.* Gene transduction efficiency and maturation status in mouse bone marrow-derived dendritic cells infected with conventional or RGD fiber-mutant adenovirus vectors. *Cancer Gene Ther* 2003; **10**(5): 421–31.
38 Kaisho T, Takeuchi O, Kawai T, Hoshino K, Akira S. Endotoxin-induced maturation of MyD88-deficient dendritic cells. *J Immunol* 2001; **166**(9): 5688–94.
39 Helmich BK, Dutton RW. The role of adoptively transferred CD8 T cells and host cells in the control of the growth of the EG7 thymoma: factors that determine the relative effectiveness and Homing properties of Tc1 and Tc2 effectors. *J Immunol* 2001; **166**: 6500–8.
40 Akazawa T, Shingai M, Sasai M *et al.* Tumor immunotherapy using bone marrow-derived dendritic cells overexpressing Toll-like receptor adaptors. *FEBS Lett* 2007; **581**(18): 3334–40.
41 Matsumoto M, Nishiguchi M, Kikkawa S, Nishimura H, Nagasawa S, Seya T. Structural and functional properties of complement-activating protein M161Ag, a Mycoplasma fermentans gene product that induces cytokine production by human monocytes. *J Biol Chem* 1998; **273**: 12407–14.
42 Nishiguchi M, Matsumoto M, Takao T *et al.* Mycoplasma fermentans lipoprotein M161Ag-induced cell activation is mediated by Toll-like receptor 2: role of N-terminal hydrophobic portion in its multiple functions. *J Immunol* 2001; **166**: 2610–16.
43 Hida T, Hayashi K, Yukishige K, Tanida S, Kawamura N, Harada S. Synthesis and biological activities of TAN-1511 Analogues. *J Antibiot* 1995; **48**(7): 589–603.
44 Reutter F, Jung G, Baier W, Treyer B, Bessler WG, Wiesmüller KH. Immunostimulants and Toll-like receptor ligands obtained by screening combinatorial lipopeptide collections. *J Pept Res* 2005; **65**(3): 375–83.
45 Gobin SJ, Peijnenburg A, Keijsers V, van den Elsen PJ. Site a is crucial for two routes of IFN g-induced MHC class I transactivation: the ISRE-mediated route and a novel pathway involving CIITA. *Immunity* 1997; **6**(5): 601–11.
46 Buerkle MA, Pahernik SA, Sutter A, Jonczyk A, Messmer K, Dellian M. Inhibition of the alpha-nu integrins with a cyclic RGD peptide impairs angiogenesis, growth and metastasis of solid tumours *in vivo*. *Br J Cancer* 2002; **86**(5): 788–95.
47 Janssen ML, Oyen WJ, Dijkgraaf I *et al.* Tumor targeting with radiolabeled alpha(v)beta(3) integrin binding peptides in a nude mouse model. *Cancer Res* 2002; **62**(21): 6146–51.
48 Seya T, Matsumoto M, Tsuji S, Begum NA, Azuma I, Toyoshima K. Structural-functional relationship of pathogen-associated molecular patterns: lessons from BCG cell wall skeleton and mycoplasma lipoprotein M161Ag. *Microbes Infect* 2002; **4**(9): 955–61.